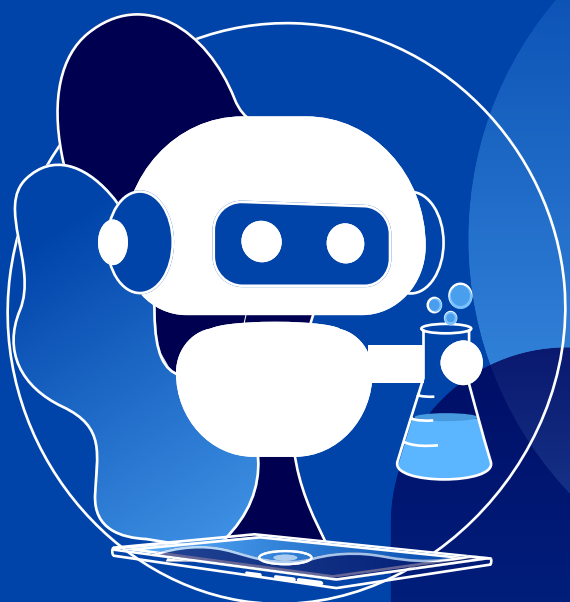




**POSTER MINUTE**

# **AI in napredne tehnologije v znanosti**

*Zbornik posterjev*



**Ljubljana, 22. oktober 2024**

Zbornik posterjev

**AI IN NAPREDNE TEHNOLOGIJE V ZNANOSTI**

Poster minute, Ljubljana, 22. oktober 2024

Poster minute se je odvijal v okviru interdisciplinarnega strokovno-izobraževalnegadogodka BEST dnevi znanosti (22. – 24. oktober 2024)

Kraj dogodka: Univerza v Ljubljani, Fakulteta za kemijo in kemijsko tehnologijo,  
Večna pot 113, 1000 Ljubljana

**Urednika:**

Deni Krašna

Lara Likar

**Organizacijski odbor:**

Zara Bunc, Neža Bajec, Špela Blaznik, Lara Likar, Tinkara Korošec, Neja Brumec, Karin Kunstelj, Lucija Kovaček, Deni Krašna, Manca Simončič, Nik Čadež

**Grafično oblikovanje:** Neža Bajec

**Založnik zbornika in organizator konference:**

Društvo BEST Ljubljana

**Kraj in leto izida:**

Ljubljana, 2024

Publikacija je izšla v elektronski obliki in je dostopna na spletnem naslovu:

<https://www.best-dnevi-znanosti.si>

Kataložni zapis o publikaciji (CIP) pripravili v Narodni in univerzitetni knjižnici v Ljubljani

[COBISS.SI-ID 218927875](#)

ISBN 978-961-96808-2-7 (PDF)

# Pravilnost odgovorov in omejitve prosto dostopnega orodja ChatGPT v slovenščini na primerih okoljske problematike

I. Kralj Cigić, T. Balaško, N. Guzelj, L. Lengar, J. Levstek, G. Pirnat, L. Stepanova, L. Šarić, J. Štenkler, K.

Ziherl, H. Prosen\*

Univerza v Ljubljani, Fakulteta za kemijo in kemijsko tehnologijo, Ljubljana, Slovenia \*helena.prosen@fkkt.uni-lj.si

## OZADJE

V novembru 2022 je podjetje OpenAI iz ZDA dalo v prosti medmrežni dostop prvo različico orodja ChatGPT (Sl. 1), ki je tako imenovani *chatbot*, torej orodje umetne inteligence (UI), ki se aktivno "pogovarja" z uporabnikom. Preko dostopa do medmrežnih virov zbira informacije, ki jih uporabniku predstavi v obliki odgovora na zastavljeno vprašanje. Omogoča pisanje daljših in kraješih besedil na želeno tematiko, obseg in vsebino pa lahko uporabnik z dodatnimi vprašanji in ključnimi besedami nadalje usmerja v želeno smer. Orodje so doslej že večkrat posodobili, na voljo pa je bodisi v preprostejši, prosto dostopni, bodisi v bolj zmogljivi plačljivi različici. Pojav orodja ChatGPT je sprožil pospešen razvoj podobnih orodij UI drugih ponudnikov.

S pojavom ChatGPT so se razvile intenzivne razprave o koristnosti oziroma škodljivosti orodij UI. V zvezi z visokošolskim izobraževanjem je pogosto izražena zaskrbljenost, da študentje svoje pisne izdelke lahko napišejo z orodji UI in da je taka zloraba neizsledljiva. Univerza v Ljubljani se je odzvala z dokumentom 'Priporočila Univerze v Ljubljani pri uporabi umetne inteligence' [1], ki navaja tako primere koristne kot neustrezne oziroma nedovoljene uporabe orodij UI.

V času od pojava ChatGPT so njegov način delovanja ter potencialno koristno uporabo v visokem šolstvu proučevali že v številnih raziskavah [2]. Čeprav je ob pravilni uporabi učinek na učni proces lahko pozitiven [2], pa podane informacije niso vedno pravilne [3]. Zlasti je potrebna previdnost pri citatih in navajanju virov, saj jih ChatGPT pretežno generira sam in niso resnične reference [3].



Slika 1: Logo ChatGPT

## ZASNOVA RAZISKAVE

Pri predmetu Kemija okolja za študente univerzitetnega študijskega programa Kemija na Fakulteti za kemijo in kemijsko tehnologijo UL so študenti preverjali pravilnost odgovorov in omejitve orodja ChatGPT na primerih vprašanj iz okoljske problematike. Nekaj podobnih raziskav je bilo že izvedenih v angleškem jeziku, predvsem v zvezi z informacijami o klimatskih spremembah [4,5] ali klimatski politiki [6], pa tudi o zmožnosti orodja, da identificira pomembne okoljske tematike, ki še niso dovolj raziskane [7].

V naši raziskavi smo se pri uporabi ChatGPT omejili na prosto dostopno, neplačljivo orodje. Vsa vprašanja, ključne besede in odgovori so bili v slovenščini. S tem smo se zelenili približati izkušnji slovenskega laičnega uporabnika. Študentje so najprej zastavili poljudno vprašanje, zatem pa zahtevali bolj strokovnen odgovor z dodajanjem specifičnih ključnih besed. Pri obeh odgovorih pa so nato preverili pravilnost s primerjavo z znanstveno literaturo.

## Vprašanje 1: Kakšen je vpliv globalne proizvodnje, predelave, dostave in potrošnje hrane na Zemeljsko klimo?

ChatGPT se je pri poljudnem sestavku osredotočil na nekaj glavnih problematik vprašanja: emisije toplogrednih plinov, deforestacija, transport, poraba vode, odpadki ter izguba biotske raznovrstnosti. Dotaknil se je torej skoraj vseh največjih problemov prehrambene industrije. Odgovori so bili sicer pretežno pravilni, vendar opisani precej površno, brez specifičnih podatkov. Odgovor je bil razumljiv tudi za laike, čeprav so se pojavili tudi strokovni izrazi, npr. »anaerobna razgradnja«, ter tukaj ali napačni direktni prevodi – primer: "rastlinjaki plini" (angl. *greenhouse gases*) namesto "toplogredni plini". Pri strokovnem odgovoru orodje ni podalo nič več podrobnosti kot pri poljudnem, temveč se je osredotočilo izrecno na razlagu ključnih besed, ki so bile dodane vprašanju.

## Vprašanje 2: Prednosti in slabosti uporabe električnih avtomobilov. Ali so električni avtomobili zares odgovor za čistejšo prihodnost?

ChatGPT v nobenem od odgovorov ni definiral, o kateri podvrsti električnih avtomobilov razpravlja (baterijska električna vozila, električna vozila z gorivno celico, hibridna električna vozila). Uporabil je predpostavko, da je bralec seznanjen s tehnično terminologijo, kar ni nujno res. Sicer pa je odgovor napisan v preprostem jeziku, primeren tudi za nezahtevne brale. Izstopa zaokroženost besedila. V strokovnem odgovoru trditev niso bile zadostno utemeljene, temveč predstavljene kot neizpodbitna dejstva. Večina besedila ni bila v protislovju z znanstvenimi dognanji, vendar tudi informativna vrednost ni bila velika. Izogib pospolištvam je orodje pogosto uporabilo trditev, da se v različnih primerih izbran parameter obravnava različno, ne da bi podalo osnovno delitev na različne primere. Izstopa fragmentirana oblika besedila in odsotnost osrednje teze. Citirani so bili članki iz uglednih znanstvenih revij, toda ob pregledu je bilo ugotovljeno, da ne obstajajo.

## RAZPRAVA IN ZAKLJUČKI

Skupna analiza poljudnih in strokovnih odgovorov, ki so jih študenti dobili z uporabo orodja ChatGPT v neplačljivi slovenski različici, je omogočila identifikacijo nekaterih prednosti in slabosti orodja za informiranje o okoljskih tematikah v slovenščini.

Prednosti so:

- omogoča hiter pregled ogromne količine informacij, dostopnih v medmrežnih virih;
- glede vsebine odgovorov je sicer zanesljiv, a precej bolj primeren za splošno (laično, nestrokovno) uporabo, ko želi uporabnik pridobiti le osnovne informacije – Sl. 2;
- lahko se uporablja za osnovno informiranje in kot izhodišče za nadaljnje raziskovanje, vendar ni zanesljiv kot vir pri kompleksnih in poglobljenih temah.

Glavne slabosti:

- ažurnost podatkov, iz katerih črpa (npr. v avgustu 2024 je baza podatkov segala do oktobra 2023);
- upošteva tudi nepreverjene medmrežne vire;
- uporaba napačnih slovenskih izrazov zaradi neposrednega in nepreverjenega prevajanja iz drugih jezikov, zlasti angleščine;
- orodje je naučeno, da prekomerno upošteva ključne besede, zato se pojavi nevarnost podajanja nepravilnih informacij, če uporabnik vztraja na izbranih zahtevah;
- odgovori so zelo splošni, mestoma tudi netočni, ter brez konkretnih podatkov;
- uporaba pravilnega standarda citiranja in verodostojnost naslova članka ter znanstvene revije učinkovito prikriva, da gre za navidezni vir, medtem ko ostajajo dejanski viri necitirani, kar izpostavlja uporabnika orodja morebitnim posledicam kršitve pravic intelektualne lastnine.

## REFERENCE

- [1] Priporočila Univerze v Ljubljani pri uporabi umetne inteligence. Dostopno na: <https://www.uni-lj.si/novice/2023-09-20-priporocila-univerze-v-ljubljani-pri-uporabi-umetne-inteligence> (dostop 21.6.2024)
- [2] M. Montenegro-Rueda, J. Fernández-Cerero, J. M. Fernández-Batánero, E. López-Meneses. *Computers* 2023, 12, 153. <https://doi.org/10.3390/computers12080153>
- [3] T. Day. *The Professional Geographer* 2023, 75, 1024-1027, DOI: 10.1080/00330124.2023.2190373
- [4] A. Krzyżewska. *Miscellanea Geographica* 2024, 28, 5-12, DOI: 10.2478/mgsrd-2023-0017
- [5] B. Sommer, S. von Querfurth. *Ambio* 2024, 53, 951-959. <https://doi.org/10.1007/s13280-024-01997-7>
- [6] F. Salekay, J. van den Berg, I. Savin. *Ecological Economics* 2024, 226, 108352. <https://doi.org/10.1016/j.ecolecon.2024.108352>
- [7] E. Agathokleous, C. J. Saitanis, C. Fang, Z. Yu. *Science of the Total Environment* 2023, 888, 164154. <http://dx.doi.org/10.1016/j.scitotenv.2023.164154>

## ZAHVALA

Avtorji se zahvaljujejo Javnim agencijam za znanstvenoraziskovalno in inovacijsko dejavnost Republike Slovenije ARIS (programski skupini P1-0153 in P1-0447), ki je finančno omogočila raziskovalno delo.

# Development of a continuous $\delta$ -viniferin synthesis in a microreactor using immobilized horseradish peroxidase

Natalija Tomažin<sup>a</sup>, Marko Božinović<sup>a</sup>, Francesca Annunziata<sup>b</sup>, Andrea Pinto<sup>b</sup>, Polona Žnidaršič-Plazl<sup>a,\*</sup>

<sup>a</sup>University of Ljubljana, Faculty of Chemistry and Chemical Technology, Večna pot 113, SI-1000 Slovenia

<sup>b</sup>Università degli Studi di Milano, Department of Food, Environmental and Nutritional Sciences, Via Celoria 2, IT-20133 Milano, Italy

\*email: polona.znidarsic@fkkt.uni-lj.si

## INTRODUCTION

$\delta$ -viniferin is a resveratrol dehydrodimer, an isomer of  $\varepsilon$ -viniferin, which widely exists in grapes, knotweed, peanuts, and red wine. It was found to have biological activities, such as antiviral, anti-inflammatory, antibacterial, anticancer, and antioxidation. It possesses strong antioxidant properties, which can help protect the body against free radicals and oxidative stress. Additionally,  $\delta$ -viniferin has been found to have anti-inflammatory properties, aiding in reducing inflammation in the body. Some researchers have also suggested that  $\delta$ -viniferin could have the potential to fight various diseases, including cancer, cardiovascular diseases, and neurodegenerative disorders.<sup>1,2</sup> However, at a cost often exceeding 300 euros for just 1 milligram, the expense associated with  $\delta$ -viniferin may severely restrict research efforts and its global applicability.

## AIM

- to develop a cost-effective and sustainable process for synthesizing  $\delta$ -viniferin from bio-derived materials using horseradish peroxidase (HRP)
- optimization of crosslinked enzyme aggregates of HRP (CLEA-HRP) generation using microfluidic system<sup>3</sup>

## EXPERIMENTAL

### Optimization of CLEA-HRP generation (Figure 1)

Optimization focused on determining the optimal residence time for precipitation and crosslinking, screening various precipitation solvents, and adjusting the glutaraldehyde (GA) concentration for enzyme crosslinking at 25°C in PTFE tubes of various lengths with 0.8 mm inner diameter. Horseradish peroxidase (HRP) was dissolved in 0.1 M potassium phosphate buffer (pH 6.0).

Residence times in a microfluidic system obtained by changing the tube's lengths: 3.77, 1.88, 0.94, 0.47 and 0.34 min

HRP inlet concentration: 0.02 mg/mL

HRP inlet solution flow rate: 50  $\mu$ L/min

Organic solvents tested for precipitation: acetone, acetonitrile, isopropanol and ethanol.

Organic solvent flow rate: 50  $\mu$ L/min

Crosslinking agent: 1, 1.5, 0.5, 0.1 mM glutaraldehyde (GA) solution

Crosslinking agent flow rate: 100  $\mu$ L/min

The size of CLEA-HRP was assessed through dynamic light scattering analysis (DLS).

The activity of CLEA-HRP was measured spectrophotometrically using ABTS test<sup>4</sup> - the activity of CLEA-HRP was compared to the free enzyme (recovered activity).

### Batch reaction<sup>5</sup> (Figure 2)

Various amounts (80 mg, 100 mg, 120 mg) of resveratrol were dissolved in 4.621 mL of citrate buffer (pH 5.0) with 50% (v/v) of acetone. 3,79% (v/v) of HRP in Milli-Q water (1 mg/mL) was added and the mixture was stirred for 30 min at tested temperature. Subsequently, 1.43% (v/v) of  $H_2O_2$  was added and the mixture was stirred for 1 h at tested temperature.

Temperature: 40°C

For quenching the reaction, the solution was placed in ice. The concentrations of resveratrol and  $\delta$ -viniferin were analyzed using HPLC with Gemini-NX 3  $\mu$ m C18 110 Å (150  $\times$  4.60 mm) column and UV/VIS detector.

### Continuous flow reaction (Figure 3): Work in progress

## RESULTS

### Optimization of CLEA-HRP generation

Table 1: Results of testing different residence times; organic solvent: pure acetone, 1 mM GA

Tube length, cm	t, min	Recovered activity, %	St. dev., %
100	3.77	74.96	3.10
50	1.88	85.48	4.13
25	0.94	93.15	2.37
12.5	0.47	93.32	1.68
9	0.34	98.36	1.67

Tube with a length of 9 cm and a residence time of 0.34 min was selected for further testing due to its highest achieved recovered activity (Table 1).

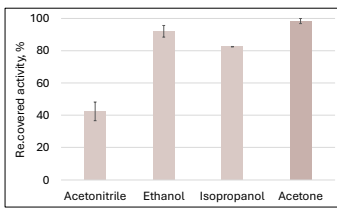


Figure 4: The effect of tested organic solvents as precipitation solvents on recovered activity; 1 mM GA, residence time 0.34 min

Acetone was selected among the tested organic solvents as the best-tested solvent for precipitation because of the highest achieved recovered activity (Figure 4).

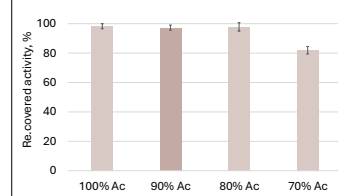


Figure 5: Results of testing different acetone:buffer ratios; 1 mM GA, residence time: 0.34 min

The final choice of organic solvent was 90% (v/v) acetone due to its highest recovered activity (Figure 5).

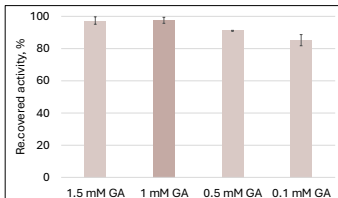


Figure 6: Results of testing different concentrations of glutaraldehyde; organic solvent: 90 vol.-% acetone, residence time 0.34 min

1 mM was selected as the best GA concentration for cross-linking because the highest recovered activity was retrained (Figure 6).

### DLS

The resulting CLEA-HRP exhibited an average particle radius of 150 nm (Figure 7).

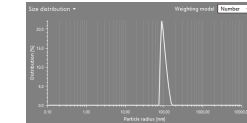


Figure 7: Size distribution of CLEA-HRP; 90% (v/v) acetone, 1 mM GA, retention time 0.34 min

### Batch reaction

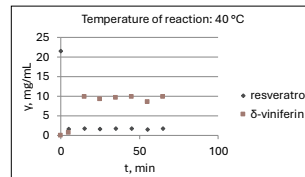


Figure 8: Concentrations of resveratrol and  $\delta$ -viniferin at 40°C, initial mass of resveratrol: 100 mg

The yield of the reaction performed in a batch process was 45.7% after 15 min (Figure 8).

### CONCLUSIONS

The highest recovered activity of 99% was achieved at a residence time of 0.34 min with acetone and glutaraldehyde concentrations of 90% (v/v) and 1 mM, respectively. The resulting CLEA-HRP exhibited an average particle radius of 150 nm.

The reaction was successfully performed with a yield of 45.7% after 15 min.

## ACKNOWLEDGEMENT

This work was supported by Slovenian Research and Innovation Agency (anis) through Grants J4-4562 and P2-0191. MB was financed through Horizon Europe MSCA Doctoral Network project GreenDigiPharma (Grant 101073089), while FA was supported by National Recovery and Resilience Plan (NRRP), Mission4 Component 2 Investment 1.3 - Call for tender No. 341 of 15/03/2022 of Italian Ministry of University and by the European Union-NextGenerationEU, in the frame of the project Research and innovation network on food and nutrition Sustainability, Safety and Security (ON Foods).

## REFERENCES

- Shang, Y.; Li, X.; Sun, T.; Zhou, J.; Zhou, H.; Chen, K. Comparative theoretical researches on the anti-oxidant activity of  $\delta$ -viniferin and  $\varepsilon$ -viniferin. *Journal of Molecular Structure* **2021**, *1245*, 131062. <https://doi.org/10.1016/j.molstruc.2021.131062>.
- Zwygart, A. C.; Medaglia, C.; Huber, R.; Poli, R.; Marcourt, L.; Schnée, S.; Michellod, E.; Mazel-Sánchez, B.; Constant, S.; Huang, S.; Bekliz, M.; Clément, S.; Gindro, K.; Queiroz, E. F.; Tapparel, C. Antiviral properties of trans- $\delta$ -viniferin derivatives against enveloped viruses. *BioMedicine & Pharmacotherapy* **2023**, *163*, 114825. <https://doi.org/10.1016/j.biopharm.2023.114825>.
- Menegatti, T.; Lavrič, Ž.; Žnidaršič-Plazl, P. Microfluidics-based preparation of cross-linked enzyme aggregates. WO2023175002A1.
- (4) <https://www.sigmal Aldrich.com/HR/en/technical-documents/protocol/protein-biology/enzyme-activity-assay-of-peroxidase-abts-as-substrate>
- (5) Mattio, L. M.; Dallavalle, S.; Musso, L.; Filardi, R.; Franzetti, L.; Pellegrino, L.; D'Incecco, P.; Mora, D.; Pinto, A.; Arioli, S. Antimicrobial Activity of Resveratrol-Derived Monomers and Dimers against Foodborne Pathogens. *Sci. Rep.* **2019**, *9* (1), 1–13.

## Understanding the mode of activation of plasmacytoid dendritic cells in different skin disorders

Neža Lesjak<sup>1</sup>, Jeremy Di Domizio<sup>1\*</sup>

<sup>1</sup>Department of Dermatology, CHUV University Hospital and University of Lausanne (UNIL), Lausanne, Switzerland

\* Corresponding authors: Jeremy.Di-Domizio@chuv.ch

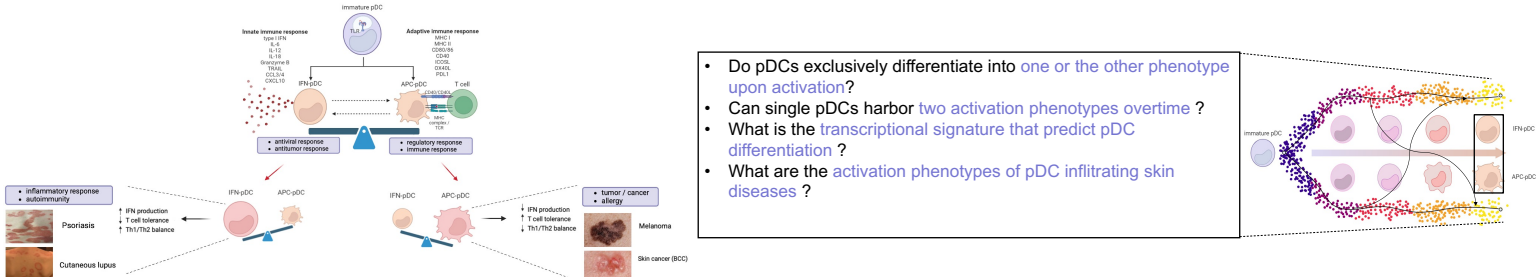
## BACKGROUND and HYPOTHESIS

Plasmacytoid dendritic cells (pDCs) are a unique dendritic cell subset which represents from 0.2 - 0.8% of human peripheral blood mononuclear cells (PBMCs). These rare circulating cells express Toll-like receptors TLR7 and TLR9 and can produce large amounts of type I interferons (IFNs) upon viral stimulation, thereby playing a critical role in linking innate and adaptive immunity (Ref 1).

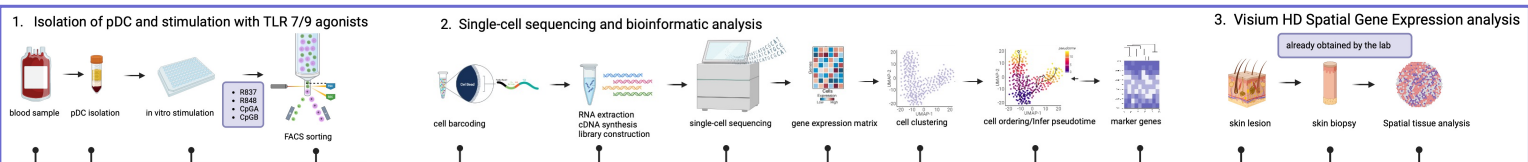
However, in inflammatory autoimmune diseases such as psoriasis and lupus, pDCs are abnormally activated. Conversely, in many cancers pDCs infiltrate tumors but produce less IFN-alpha, promoting immune suppression and tumor growth (Ref 2).

PDCs have shown phenotypic heterogeneity upon activation leading to two distinct populations: IFN production (IFN-pDCs) or antigen-presenting capacities (APC-pDCs). However, pDC differentiation into these two distinct types remains poorly understood.

We hypothesized that plasmacytoid dendritic cell diversification upon activation leads to two main phenotypes named IFN-pDC and APC-pDC, that can be predicted by the identification of specific transcriptional modules using scRNAseq.

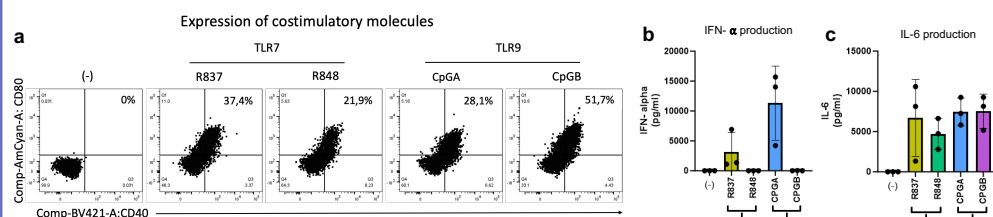


## METHODS



## PRELIMINARY RESULTS

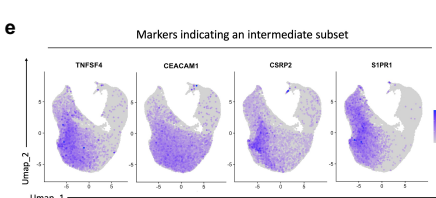
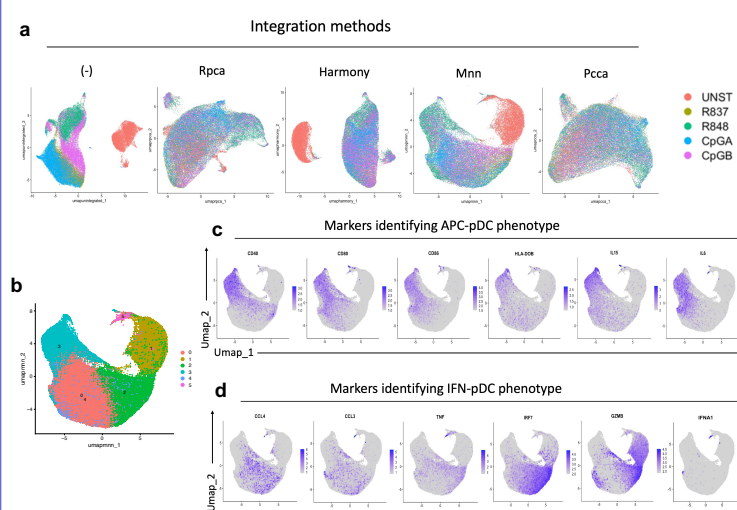
## 1. Verifying pDC phenotypes upon stimulation with four different agonists



To determine whether plasmacytoid dendritic cells (pDCs) exhibit distinct phenotypic profiles in response to different stimuli, we stimulated freshly isolated pDCs using Imiquimod (R837), Resiquimod (R848), CpG4, and CpG8. The cells were subsequently analyzed using surface markers including IFN- $\alpha$ , CD40, CD80, and CD83. Our results indicate the presence of an antigen-presenting cell (APC)-like phenotype following stimulation with CpGB (a TLR-9 agonist) and R837 (a TLR-7 agonist) (Fig. 1a). To further investigate cytokine production, a cytometric bead array (CBA) was performed to detect interferon signalling, utilizing antibodies against IFN- $\alpha$  and IL-6. Notably, we observed that stimulation with R837 not only promoted an APC signature but also led to the production of IFN- $\alpha$ . This suggests a potential role for scRNA-seq in further elucidating the distinction between TLR agonist responses (Fig. 1b). In addition to IFN type I production, pDCs demonstrated IL-6 expression, indicating cellular activation and maturation (Fig. 1c).

In summary, these data demonstrate that the two phenotypes (IFN and APC) can be obtained following stimulation with different TLR-7/9 agonists.

## 2 Identifying the subsets in single cell RNA sequencing

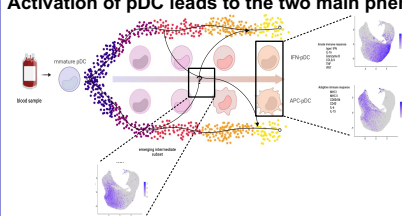


Following single-cell RNA sequencing of pDCs stimulated for 24 hours, we employed various bioinformatic tools to identify cellular subsets. After testing different markers, minimum neighbor (MNN) integration was selected to produce a more suitable database for transcriptomic similarity when visualized via UMAP. We employed a clear separation of clusters corresponding to cells treated with different TLR agonists (Fig. 2a). We then wanted to characterize the different clusters (Fig. 2b). We found that cluster 3 expressed APC markers: HLA-DOB, CD80, CD40, CD86, IL-15, IL-6 (Fig. 2c). Cluster 2 expressed markers of the IFN- $\beta$  phenotype: CCL4, CCL3, TNF, IFN7, GZMB and IFNA-1. Interestingly, IL-6 was nearby (Fig. 2d). Upon further analysis of the most representative markers within MNN-derived clusters, we identified an emerging pDC subset characterized by an intermediate expression profile, clustering between the two primary subsets: APC-pDCs and IFN-pDCs. This newly classified intermediate subset is defined by the expression of four prominent markers: TNFSF4, CEACAM1, CSRP2, and S1PR1 (Fig. 2e). These markers are well-known for their roles in mediating cellular adhesion, immune interactions, and functions related to cell proliferation, adhesion, and migratory capacity.

These findings demonstrate that the two subsets (APC-pDC and IFN-pDC) of pDCs can be distinguished at the single cell level, suggesting that they harbor different transcriptomes. Moreover, we observed an emerging third subset that might be an intermediate stage during pDC differentiation.

## SUMMARY

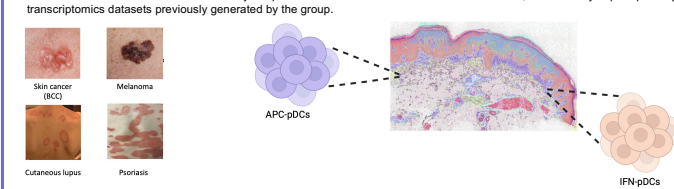
Activation of  $\alpha$ DC leads to the two main phenotypes, APC- $\alpha$ DC and IFN- $\alpha$ DC.



- Activation of plasmacytoid dendritic cells with TLR 7/9 agonists leads to the two main phenotypes APC-pDC and IFN- $\alpha$ +
  - An emerging third intermediate phenotype that express adhesion and migration markers could be the link between the two subsets

ONGOING RESEARCH

- To be able to track pDC differentiation over time, we will add another timepoint at 6h.
  - To confirm our results *in vivo* and to identify the pDC subsets that infiltrate different skin diseases, we will analyze pDC phenotypes in spatial



# Bioconjugation and covalent binding of native proteins using azide-alkyne cycloaddition

Nadja Suhorepec<sup>a</sup>, Luka Ciber<sup>a</sup>, Uroš Grošelj<sup>a</sup>, Bogdan Štefane<sup>a</sup>, Marko Novinec<sup>a</sup>, Jurij Svetec<sup>a</sup>

<sup>a</sup> University of Ljubljana Faculty of Chemistry and Chemical Technology, Večna pot 113, SI-1000 Ljubljana

## INTRODUCTION

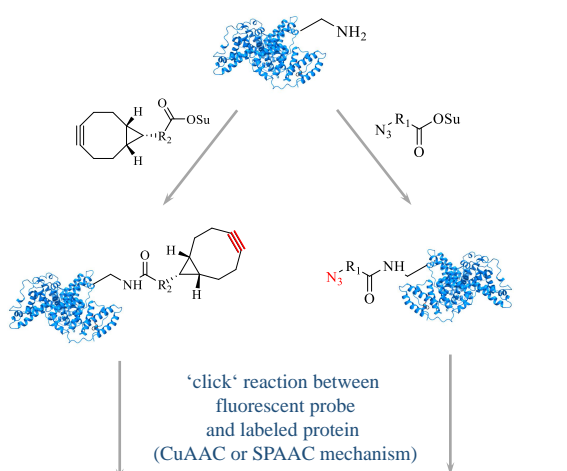
~ Bioconjugation reactions are bioorthogonal reactions in which a covalent bond is formed between two molecules, one of which is a biological molecule or its fragment. [1] Such bioorthogonal reactions are also suitable for chemical cross-linking of proteins. [2]

~ We developed a protocol for binding NHS esters, maleimides and benzotriazolides that are functionalized with either an azide group or a cyclooctyne group to proteins (lysine or cysteine residues) and an analytical method for quantifying the binding (loading) to proteins. [3]

## STRATEGY

### Step 1:

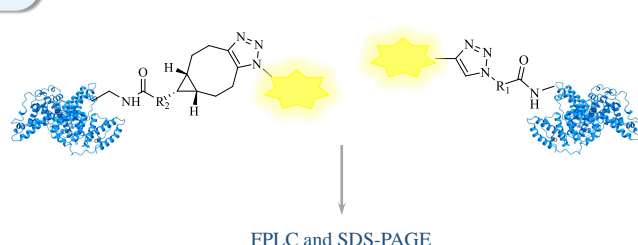
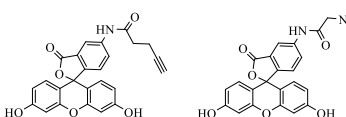
Bioconjugation of tags with two complementary bioorthogonal groups (azide and cyclooctyne group, separately) to the protein.



### Step 2:

Spectrophotometrical determination of loading of each bioorthogonal groups with fluorescein derivatives.

Fluorescent probes:

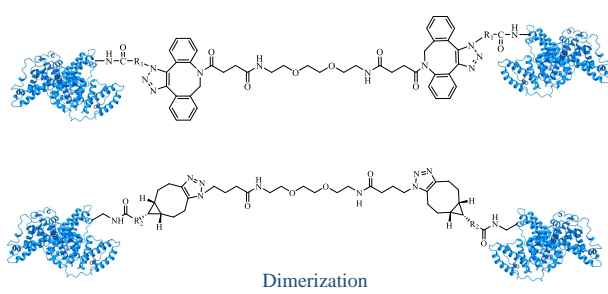
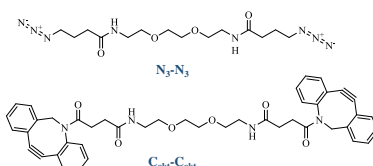


FPLC and SDS-PAGE

### Step 3:

Determination of optimal length of a linker for desired cross-linking.

Bifunctional reagents that act as intermediate connectors:



## CONCLUSION

We successfully prepared various NHS esters, benzotriazolides and maleimides that were functionalized with either an azide group or a cyclooctyne group. We developed a protocol for binding these molecules to proteins and an analytical method for quantifying the loading. With known loading of labels on the protein in hand, we were able to perform experiments on protein dimerization via azide-cyclooctyne [3+2] cycloaddition reaction. To extend the linker, we prepared bifunctional reagents that could act as intermediate connectors of the two protein molecules.

## References:

- [1] G. T. Hermanson: Introduction to Bioconjugation. In: Bioconjugate Techniques; Elsevier, 2013; pp 1–125.
- [2] N. Forte, M. Livano, E. Miranda, M. Morais, X. Yang, V. S. Rajkumar, K. A. Chester, V. Chudasama, J. R. Baker: Tuning the Hydrolytic Stability of Next Generation Maleimide Cross-Linkers Enables Access to Albumin-Antibody Fragment Conjugates and Tri-SFVs. *Bioconjugate Chem.* 2018, 29, 486–492.
- [3] J. Dommerholt, S. Schmidt, R. Temming, L. J. A. Hendriks, F. P. J. T. Rutjes, J. C. M. Van Hest, D. J. Lefebvre, P. Friedl, F. L. Van Delft: Readily Accessible Bicyclononyne for Bioorthogonal Labeling and Three-Dimensional Imaging of Living Cells. *Angew. Chem. Int. Ed.* 2010, 49, 9422–9425.

## Contact:

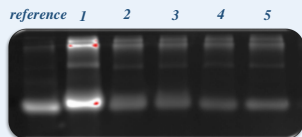
[suhorepec.nadja@gmail.com](mailto:suhorepec.nadja@gmail.com)

LinkedIn: Nadja Suhorepec

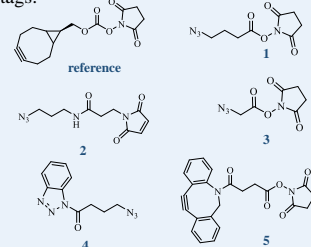
## RESULTS

SDS-PAGE gels:

- obtained after reaction between BSA, labeled with tags ref, 1–5, and fluorescent probes and scanned for fluorescein fluorescence:



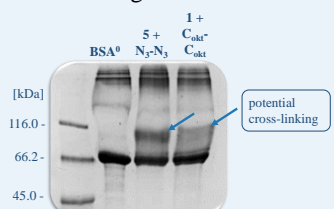
Used tags:



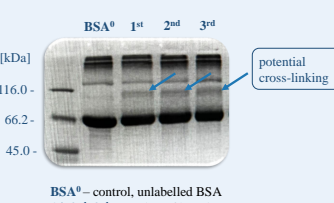
Tag	Average number of bound tags per protein molecule
reference	2.190
1	4.630
2	0.911
3	0.467
4	0.429
5	0.611

attempts at dimerization

- obtained after attempted dimerization using a single intermediate bifunctional reagent:



- obtained after iterative addition of bifunctional reagents to determine the optimal linker length for desired dimerization:



BSA<sup>0</sup> – control, unlabelled BSA

1<sup>st</sup>, 2<sup>nd</sup>, 3<sup>rd</sup> – number of iteration

# STUDY OF THE DESORPTION OF NANOPARTICLES PREVIOUSLY ADSORBED ON POLYETHYLENE MICROPLASTICS

Tjaša Likeb<sup>1</sup>, Ula Rozman<sup>1</sup>, Jernej Imperl<sup>1</sup>, Gabriela Kalčíková<sup>1</sup>

<sup>1</sup>Faculty of Chemistry and Chemical Technology, University of Ljubljana, Večna pot 113, SI-1000 Ljubljana, Slovenia  
tjasa.likeb@gmail.com

## INTRODUCTION

Microplastics (1-1000  $\mu\text{m}$ ) are introduced into the environment through various pathways, with wastewater being one of the primary sources. In wastewater, microplastics can adsorb various pollutants, including nanoparticles. These nanoparticles can later desorb in the digestive tracts of organisms, potentially causing harmful effects.

## MATERIALS & METHODS

- Nanoparticles  $\text{TiO}_2$  and  $\text{ZnO}$  (100 mg/L) were adsorbed on polyethylene microplastics.
- Desorption was studied at pH values of 6 and 8.3, with conditions including shaking at 170 rpm, and sampling at intervals of 3, 6, 12, and 24 hours. Nanoparticle concentrations were determined using ICP-MS and ICP-OES techniques.
- The desorption kinetics were analyzed using various Lagergren kinetics models, including first-order, pseudo-first-order, and pseudo-second-order models.

## INTERACTIONS

- Initial concentration of adsorbed nanoparticles on microplastics:  
 $c(n\text{TiO}_2) = 923,7 \mu\text{g/g}$   
 $c(n\text{ZnO}) = 284,2 \mu\text{g/g}$
- The maximum desorption for  $n\text{TiO}_2$  was reached after 6 h (Figure 1) and for  $n\text{ZnO}$  after 24 h (Figure 2).

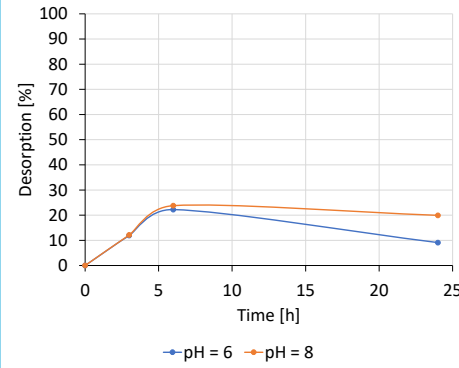


Figure 1: The desorption of  $n\text{TiO}_2$  with time

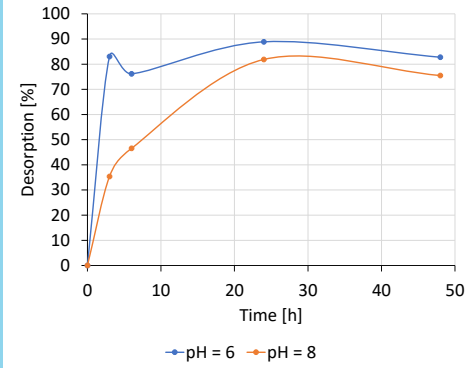


Figure 2: The desorption of  $n\text{ZnO}$  with time

## DESORPTION KINETICS

Table 1: Parameters for the pseudo-second-order kinetic model

	pH [ / ]	$K_2$ [g/ $\mu\text{g}\cdot\text{h}$ ]	$W_{e,\text{cal}}$ [ $\mu\text{g/g}$ ]	$W_{e,\text{exp}}$ [ $\mu\text{g/g}$ ]	$R^2$ [ / ]
$\text{TiO}_2$	6	0,00277	666,7	718,4	0,9977
	8	0,00336	666,7	704,0	0,9983
$\text{ZnO}$	6	0,0129	28,9	31,6	0,9833
	8	0,00536	45,0	51,5	0,9754

- $K_2$  pseudo-second-order rate constant [ $\text{g}/\mu\text{g}\cdot\text{h}$ ]  
 $W_{e,\text{cal}}$  calculated desorbed concentration at equilibrium [ $\mu\text{g/g}$ ]  
 $W_{e,\text{exp}}$  experimentally determined desorbed concentration at equilibrium [ $\mu\text{g/g}$ ]  
 $R^2$  The coefficient of determination [ / ]

## CONCLUSIONS

The study investigated the impact of pH on the desorption of nanoparticles adsorbed onto microplastics. The desorption kinetics for both  $n\text{TiO}_2$  and  $n\text{ZnO}$  nanoparticles were accurately modeled using the pseudo-second order Lagergren model, with a coefficient of determination ( $R^2$ ) near unity. The findings indicated that pH did not influence the quantity of nanoparticles desorbed. However, the kinetic rate constants revealed that both nanoparticles desorbed more quickly at lower pH levels.

# Izražanje in izolacija proteina

## fenilalanin tRNA-sintetaze (FARS)

Špela Rapuš<sup>1,\*</sup>, mag. Urša Čerček<sup>2</sup>, prof. dr. Boris Rogelj<sup>1,2,\*</sup>

1: Univerza v Ljubljani, Fakulteta za kemijo in kemijsko tehnologijo, 2: Institut Jožef Stefan, Oddelek za biotehnologijo

### Uvod

- Razširjena mutacija G4C2 na genu *c9orf72* po več mehanizmih vpliva na razvoj nevrodegenerativnih bolezni kot sta ALS in FTD.
- Protismerni prepis RNA se veže na protein FARS, kar vodi v inhibicijo aminoacilacije tRNA<sup>Phe</sup> in upad zastopanosti fenilalanina v proteomu.
- Za boljše razumevanje načina vezave in interakcije smo protein FARS izrazili v *E.coli* BL21[DE3] in izolirali.

### Metode

- Transformacija bakterij,
- izražanje rekombinantnih proteinov,
- NaDS-PAGE,
- prenos western in barvanje s Coomassie Blue,
- PCR,
- agarozna gelska elektroforeza,
- čiščenje produktov PCR,
- molekulska kloniranje z Gibsonovo reakcijo,
- izolacija plazmidov,
- restriktijska analiza in določanje nukleotidnega zaporedja,
- izolacija proteina.

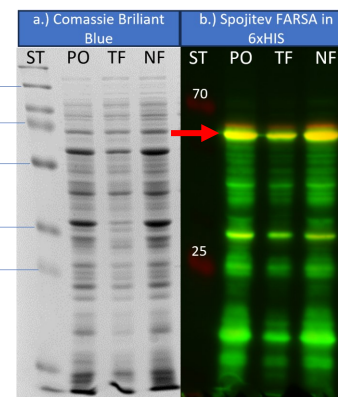
### Zaključek

- Obe podenoti proteina FARS smo uspeli izraziti v *E. coli* v zadostni količini
- FARS se boljše izraža pri nižji temperaturi, skupaj s fuzijskim partnerjem MBP
- FARS smo uspeli izolirati v manjši količini z afinitetno kromatografijo.
- V prihodnosti bi morali optimizirati postopek izolacije in izvesti študije interakcije z RNA

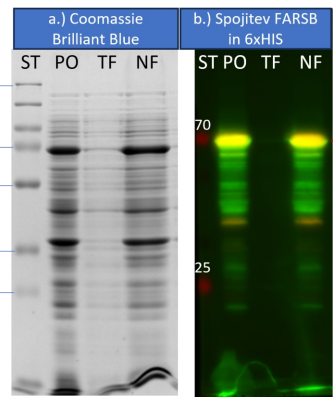
### Rezultati in diskusija

#### Izražanje pri 18 °C

Po izražanju pri 23 °C (ni prikazano) smo FARS izražali pri 18 °C, da bi dobili več proteina v topni frakciji. Podenoto FARSA smo dobili nekaj več v topni frakciji medtem ko podenote FARSB v topni frakciji nismo zaznali.



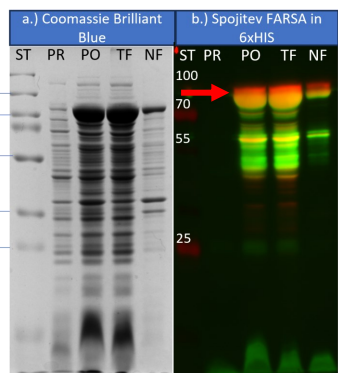
Slika 1: a) vsi proteini barvani s CBB, b) imunodetekcija proti FARSA in heksahistidinski oznaki



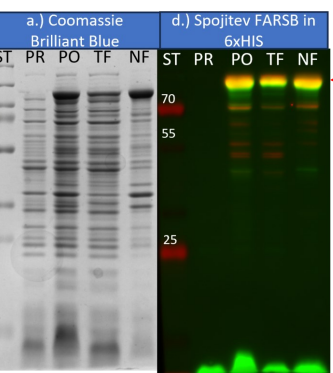
Slika 2: a) vsi proteini barvani s CBB, b) imunodetekcija proti FARSB in heksahistidinski oznaki

#### Izražanje pri 18 °C z dodanim MBP (maltoza vezavni protein)

Fuzijski partner MBP pomaga pri zvijanju proteina, da ga tako nastane več v topni frakciji. Podenoto FARSA smo uspeli v 90 % izraziti v topni frakciji, FARSB pa 50 %.



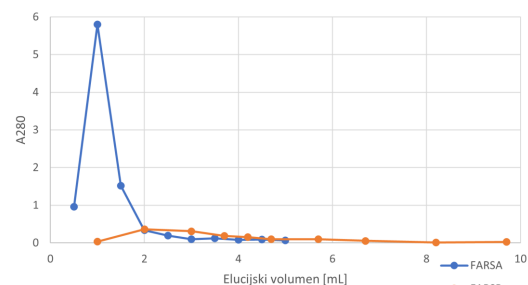
Slika 3: a) vsi proteini barvani s CBB, b) imunodetekcija proti FARSA in heksahistidinski oznaki



Slika 4: a) vsi proteini barvani s CBB, b) imunodetekcija proti FARSB in heksahistidinski oznaki

#### Poskusna izolacija

Graf odvisnosti A280 od elucijskega volumena



### Viri

\*korespondenčni avtor: boris.rogelj@ijs.si, × spela.rapus@gmail.com

- [1] M. DeJesus-Hernandez, I. R. Mackenzie, B. F. Boeve, A. L. Boxer, M. Baker, N.J. Rutherford, A. M. Nicholson, N. C. A. Finch, H. Flynn, J. Adamson, et al.: Expanded GGGGCC hexanucleotide repeat in noncoding region of C9ORF72 causes chromosome 9p-linked FTD and ALS. *Neuron* 2011, 72, 245–256.
- [2] R. Balendra, A. M. Isaacs: C9orf72-mediated ALS and FTD: multiple pathways to disease. *Nat Rev Neuro* 2018, 14, 544–558.
- [3] J. P. Taylor, R. H. Brown, D. W. Cleveland: Decoding ALS: from genes to mechanism. *Nature* 2016, 539, 197–206.



Lena Kogoj<sup>1,2</sup>, Dr. Emmanouil Kyriakakis<sup>1</sup>, Prof. Anne Spang<sup>1</sup>

1. The Biozentrum, University of Basel, Basel, Switzerland

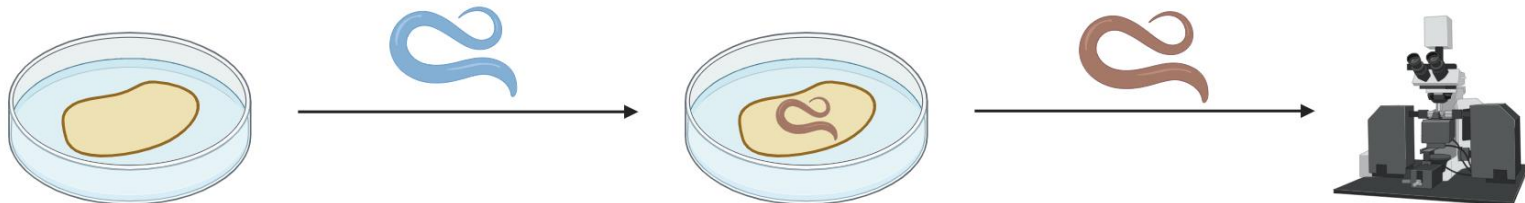
2. Fakulteta za kemijo in kemijsko tehnologijo, Univerza v Ljubljani, Ljubljana, Slovenija

## UVOD

Staranje je časovno odvisen funkcionalni upad. Znanstveniki so z raziskavami molekularnih mehanizmov staranja uspeli določiti devet znakov staranja (angl. *hallmarks of aging*), ki skupaj določajo fenotip staranja<sup>1</sup>. En od aspektov staranja je tudi izguba proteostaze ali homeostaze proteinov, ki ima lahko za posledico razvoj degenerativnih bolezni, kot sta Alzheimerjeva in Parkinsonova bolezen. Izguba proteostaze pomeni, da se proteini ne uspejo pravilno zviti in zato ne morejo upravljati svoje funkcije, pride pa tudi do njihove agregacije. Da se to ne bi dogajalo, je v celici prisotno kompleksno omrežje, ki zagotavlja proteostazo. Cilj raziskave je bil določiti, ali zmanjšanje izražanja transteritinu-podobnih proteinov (v nadaljevanju ttr) poveča število proteinskih agregatov v *C. elegans*, kar bi lahko pomenilo, da so ttr del proteostaznega omrežja<sup>2</sup>.

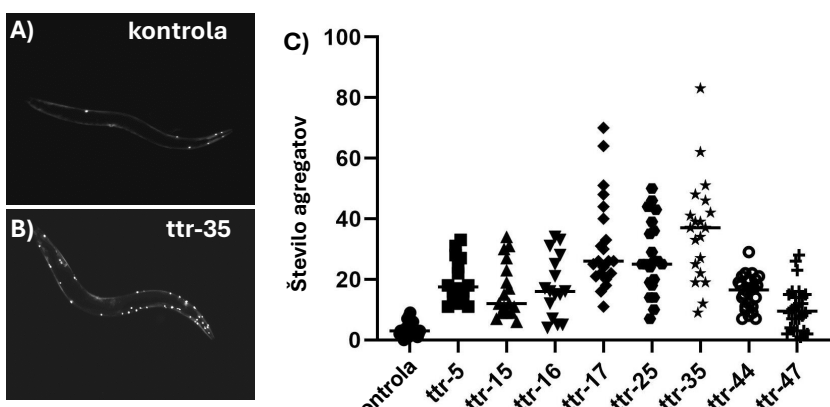
## RAZPRAVA IN REZULTATI

### Shematski prikaz poteka dela



Slika 1: Zmanjšanje izražanja genov z uporabo metode RNA-interferenca. Uporabljen je bil sev AM141, pri katerem se morebitni proteinski agregati zaradi oznake z YLP vidijo pod fluorescenčnim mikroskopom. Vključenost v proteostazno omrežje smo preverjali za ttr-5, ttr-15, ttr-16, ttr-17, ttr-25, ttr-37 in ttr-44. RNA-interferenca je bila izvedena tako, da se je vsak vzorec *C. elegans* hranil z *E. coli* z vstavljenim plazmidom za zmanjšanje izražanja gena za specifičen ttr. Povečanje števila agregatov po zmanjšanju izražanja specifičnega ttr nakazuje na vpletenost tega ttr v proteostazno omrežje.

### Rezultati RNA-interference



Slika 2: A) Mikrofotografija kontrole – brez RNA-interference. B) Mikrofotografija po RNA-interferenci za zmanjšane količino ttr-35. C) Graf števila agregatov v odvisnosti od specifičnega ttr, čigar sinteza je bila zmanjšana z RNA-interferenco.

Zmanjšanje izražanja genov za prav vse izbrane ttr poveča število agregatov napram kontroli v *C. elegans*, kar nakazuje na to, da bi ttr lahko bili del proteostaznega omrežja. Največja korelacija je vidna pri ttr-35, najmanjša pa pri ttr-47.

## ZAKLJUČEK IN UGOTOVITVE

Pokazali smo, da bi transteritinu-podobni proteini lahko igrali vlogo v proteostaznem omrežju, katerega naloga je preprečevanje agregacije proteinov.

Ne ve pa se še, na kakšen način bi ttr to lahko počeli – lahko bi namreč pomagali pri translaciji, zvitju proteinov (šaperoni) ali pa pri razgradnji nepravilno zvitih proteinov (proteaze / pot ubikvitin-proteasom / avtofagija)<sup>2</sup>.

## REFERENCE

1. López-Otín, C.; Blasco, M. A.; Partridge, L.; Serrano, M.; Kroemer, G. The Hallmarks of Aging. *Cell* **2013**, *153* (6), 1194–1217. <https://doi.org/10.1016/j.cell.2013.05.039>.
2. Hipp, M. S.; Kasturi, P.; Hartl, F. U. The Proteostasis Network and Its Decline in Ageing. *Nat. Rev. Mol. Cell Biol.* **2019**, *20* (7), 421–435. <https://doi.org/10.1038/s41580-019-0101-y>.



# OPTIMISATION OF PROTEIN PRODUCTION IN FREESTYLE 293-F CELLS WITH SIX PEPTONES

Milena Stojkovska Docevska

University of Ljubljana, Faculty of Chemistry and Chemical Technology

**ABSTRACT**

The FreeStyle™ 293-F cells were utilized to optimize proDPPI expression using six different peptones, including plant-based peptones and animal-derived Tryptone N1.

The goal of the study was to evaluate the effectiveness of these peptones in producing the proDPPI-Twin-Strep-tag construct from FreeStyle™ 293-F cells, conducted in suspension flasks.

Results revealed that peptones derived from guar, soy, and pea proteins improved protein production by approximately eightfold compared to the control without added peptones. The plant-based peptones used were G115, S146B, and P112.

**MATERIALS AND METHODS****EXPRESSION SYSTEM**

- Cells: FreeStyle™293-F suspension cells
- Vector: pDSG-IBA104
- Protein: DPPI-Dipeptidyl-peptidase I

**MEDIA COMPOSITION**

- FreeStyle 293 Expression Medium (12338026)
- 0.5% Peptones

**C-CELL PEPTONES**

- Tryptone N1 (#19553) of animal origin
- C-CELL P112, (#17112) and P118, (#17118) of pea origin
- G115, (#17115) of guar origin
- S204, (#17204) and S146B (#E0003) of soy origin

**PRE-CULTURE**

Before transfection, pre-culture of cells.

**PROTEIN EXPRESSION**

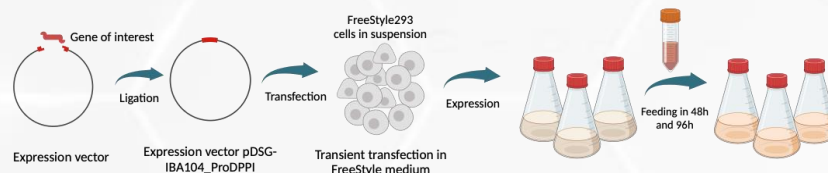
- Transfection with pDSG-IBA104 plasmid.
- Feeding with 0,5% peptones at 48h and 96 h.
- Sample collection at 120h.

**SDS-PAGE AND WB**

Coomassie staining;  
Western blot, HRP-streptavidin antibody.

**QUANTIFICATION**

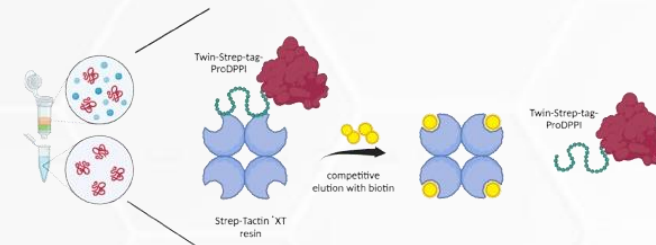
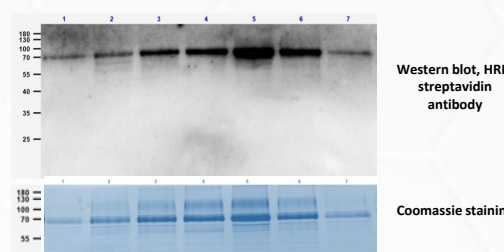
Quantification of pro DPPI in the conditioned medium from Western blot by using Bio-Rad Image lab 6.1

**INTRODUCTION**

Producing proteins in the right quantity and quality is a crucial need in modern times. The use of mammalian cells for protein production has notably increased due to their ability to ensure proper protein folding, post-translational modifications, and product assembly, all of which are vital for full biological activity. The ultimate goal of process development in animal cell culture is to increase product quality and yield while reducing cost.

Serum is essential for cell growth but is costly, inconsistent, and poses contamination risks. To address this, plant-based hydrolysates, rich in amino acids, vitamins, and peptides, are gaining popularity as serum alternatives. They not only support cell growth but also improve protein quality and reduce production costs. Overall, hydrolysates offer a promising solution to replace animal serum in cell culture.

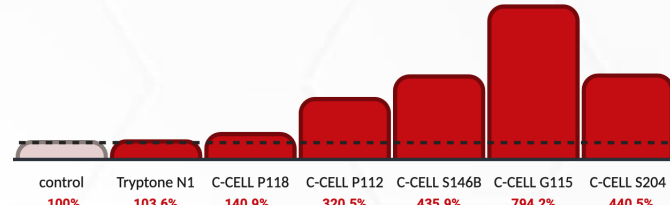
In our study, we expressed the proDPPI protein from FreeStyle™ 293-F cells five different plant-based protein hydrolysates. To enhance protein solubility and purification efficiency, we employed the Twin-Strep-tag for this experiment.

**RESULTS****Protein expression detection by SDS-PAGE and Western-blot analysis**

Western blot, HRP-streptavidin antibody  
Coomassie staining

Line	Peptone 0,5%	Expression volume/ mL	Cell density/ cells/mL	A280 nm	Mass [µg/mL]*
1	Tryptone N1	25	1,25 x10 <sup>6</sup>	0,060	36
2	C-CELL P118	25	1,25 x10 <sup>6</sup>	0,140	83
3	C-CELL P112	25	1,25 x10 <sup>6</sup>	0,200	119
4	C-CELL S146B	25	1,3 x10 <sup>6</sup>	0,245	145
5	C-CELL G115	25	1,3 x10 <sup>6</sup>	0,250	148
6	C-CELL S204	25	1,1 x10 <sup>6</sup>	0,160	95
7	Control	25	1,25 x10 <sup>6</sup>	0,043	25

\*The mass was calculated from the measured absorbance at 280 nm on NanoDrop and the amino acid sequence of the protein with the tags.

**Quantification of pro-DPPI in the conditioned medium from Western-blot****DISCUSSION AND CONCLUSIONS**

A proDPPI expression study was conducted to assess the ability of various peptones to enhance protein production yields. Different peptones were compared to standard expression without supplementation, with the protein secreted into the culture medium. The results indicated that plant-derived peptones significantly boosted proDPPI secretion compared to the control.

After purification via affinity chromatography, protein quantification was done using absorbance at 280 nm, and Western blot provided semi-quantitative analysis. Peptones enhanced the protein production by approximately eightfold compared to the control, particularly C-CELL G115, C-CELL S146B and P112 also showed more significant increase in protein production. All six peptones dissolved easily in a preheated expression media.

**ACKNOWLEDGEMENTS**

We would like to extend our special thanks to **Organotechnie SAS** for their invaluable support and the provision of peptones, which greatly contributed to the success of this study. Your collaboration has been crucial for the research, and we sincerely appreciate your contribution.

# Tissue-specific element profiles in edible seeds

Blaž Režonja<sup>1</sup>, Ela Vavpetič<sup>1</sup>, Neža Kokalj<sup>1</sup>, Aleš Kladnik<sup>1</sup>, Primož Vavpetič<sup>2</sup>, Mitja Kelemen<sup>2</sup>, Paula Pongrac<sup>1,2</sup>

<sup>1</sup> Biotechnical Faculty, University of Ljubljana, Jamnikarjeva 101, 1000 Ljubljana, Slovenia

<sup>2</sup> Jožef Stefan Institute, Jamova 39, 1000 Ljubljana, Slovenia

Jožef Stefan Institute

F2 / Department of Low and Medium Energy Physics



## INTRODUCTION

Optimising nutritional yield of existing farmland to feed the increasing global population can be achieved through biofortification [1]. Staple foodstuff, mainly seeds, differ in their element profiles and their distribution can importantly influence the success of biofortification, food processing and diets worldwide. Elemental profiles of tissues in seeds of six nutritionally important dicots (Figure 1) were captured using micro-PIXE. A five-step workflow (Figure 2) was followed: after manual sectioning, microscopy discerned tissues in seeds (Figure 3), distribution analysis depicted tissue-specific allocations of essential elements (Figure 4 disclosing results for Ca, Fe and Zn), image analysis provided their tissue-specific concentrations (Figure 5), and, ultimately, led to the estimation of nutritional potential of each seed (Table 1).

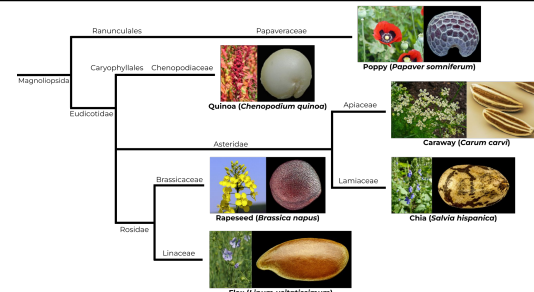


Figure 1:  
Taxonomic relationships  
of selected dicot seeds.

## RESULTS

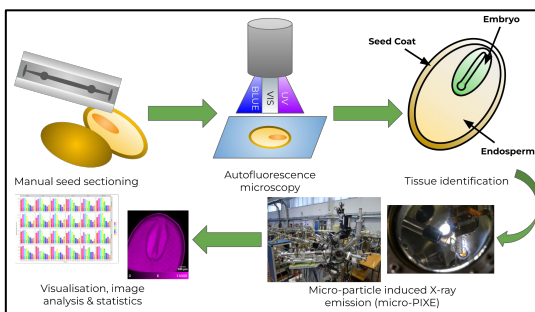


Figure 2: Workflow with key methods.

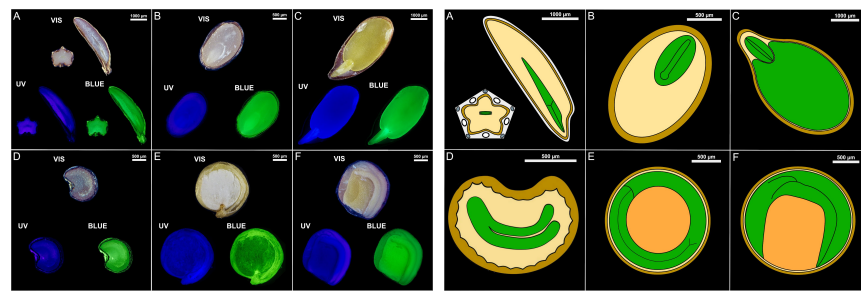


Figure 3: Autofluorescence microscopy of seed cross-sections under white (VIS) and ultraviolet (UV) excitation light (left) and microscopy-derived seed cross-section diagrams with colour-coded tissues distinguished: seed coat (brown), endosperm (beige), endosperm (green), perisperm (orange) and auxiliary structures (gray) (right). The displayed seeds are caraway (A), chia (B), flax (C), poppy (D), quinoa (E) and rapeseed (F).

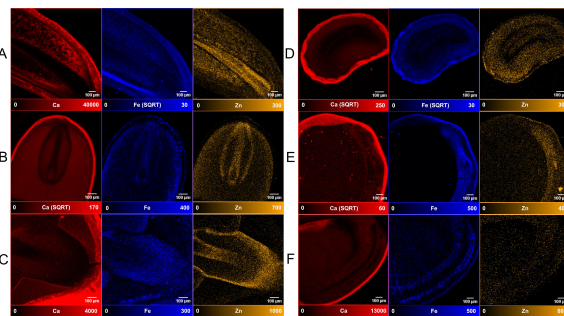


Figure 4: Micro-PIXE localisation maps of Ca, Fe and Zn. Values on colour scales are in mg kg<sup>-1</sup> dry matter. (SQR<sup>T</sup>) marks scales of square-rooted concentration values. The displayed seeds are caraway (A), chia (B), flax (C), poppy (D), quinoa (E) and rapeseed (F).

Table 1: Calculated minimum daily intake for adult males and females with all essential elements assumed to be fully bioavailable.

Element	Species	Concentration [mg kg <sup>-1</sup> ]	Male RD <sup>I</sup> [mg]	Female RD <sup>I</sup> [mg]	Male Daily Intake [g]	Female Daily Intake [g]
Ca	Caraway	5730			183	
	Chia	3393			309	
	Flax	2326			451	
	Poppy	7818	1050		134	
	Quinoa	518			2025	
Fe	Rapeseed	3096			339	
	Caraway	92			109	190
	Chia	82			123	215
	Flax	118	10	17.5	85	149
	Poppy	69			144	252
Zn	Quinoa	75			133	232
	Rapeseed	74			134	235
	Caraway	57			166	123
	Chia	84			114	84
	Flax	165	9.5	7	58	43
	Poppy	41			234	173
	Quinoa	60			157	116
	Rapeseed	55			173	128

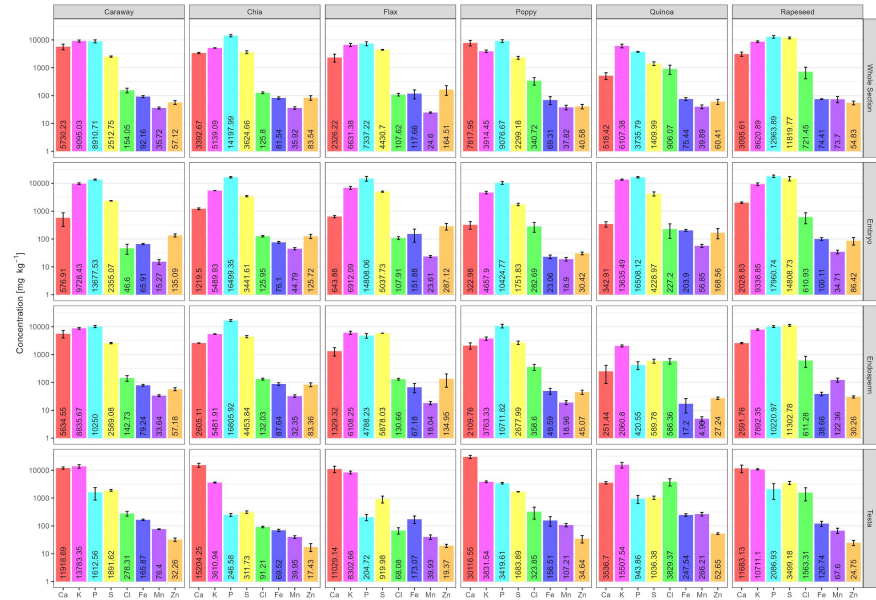


Figure 5: Whole-section and tissue-specific (embryo, endosperm and testa) element concentrations in all six seeds analysed. Note: The concentrations in mg kg<sup>-1</sup> are displayed on a logarithmic scale.

## CONCLUSIONS

- Substantial differences in Ca, Fe and Zn concentrations between species and seed tissues were found.
- In general, whole grain concentrations follow the order: P > K > S > Ca > Cl > Fe > Zn > Mn.
- Of the studied seeds, poppy seed contained the highest concentrations of Ca (allocated to the seed coat, as in other seeds) and the highest concentrations of Fe and Zn were measured in flax seeds (Fe allocated to the seed coat and Zn to the embryo).
- The elemental profiles of the endosperm and embryo in all studied dicot seeds were quite similar, which is in contrast to observations in monocot cereal grains [2].
- Data on essential element distributions in different seeds and their tissues has the potential to support informed decisions in food processing and diets worldwide.

## Bibliography

1. P. J. White & M. R. Broadley, New Phytologist. 2009, 182, 49–84.

2. A. Dettberbeck, P. Pongrac, S. Rensch, S. Reuscher, M. Pečovnik, P. Vavpetič, P. Pelicon, S. Holzheu, U. Krämer, S. Clemens, New Phytologist. 2016, doi: 10.1111/nph.13987

## Acknowledgements



Slovenian Research and Innovation Agency

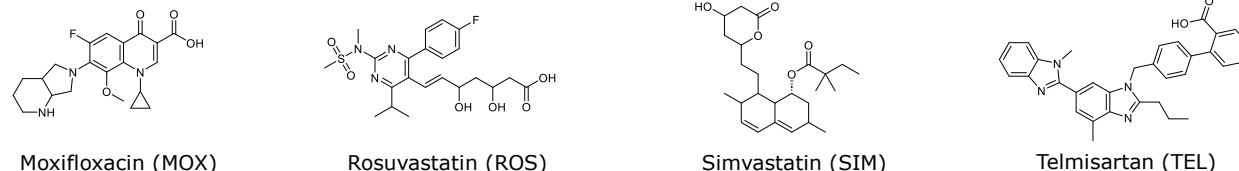


This work was supported by the Slovenian Research and Innovation Agency (through research core funding [No. P1-0112, P1-0212 and P1-0034] and project funding [J4-3091]) and the Infrastructural Centre Microscopy of Biological Samples..

# Simplified and fast analysis of selected pharmaceuticals with dispersive micro solid-phase extraction (DMSPE)

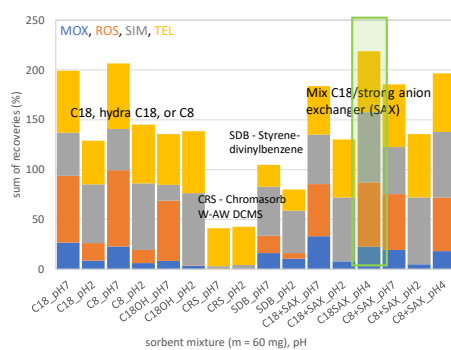


## Unveiling practical aspects of DMSPE-HPLC-UV for analysis of 4 selected pharmaceuticals



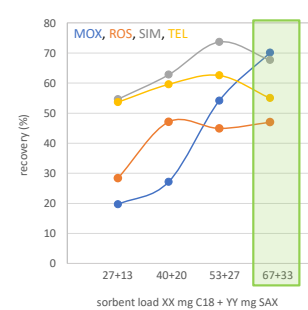
## RESULTS

### 1) Sorbent screening



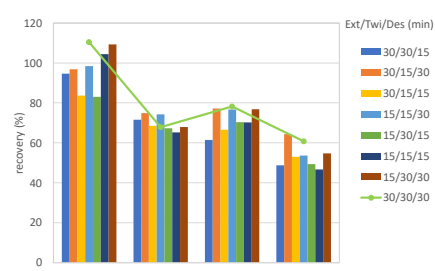
The C18 and C8 sorbents (pH 7) provided the highest recoveries. However, addition of SAX and creation of mixture C18/SAX even increased efficiency, especially at pH 4.

### 2) Sorbent load



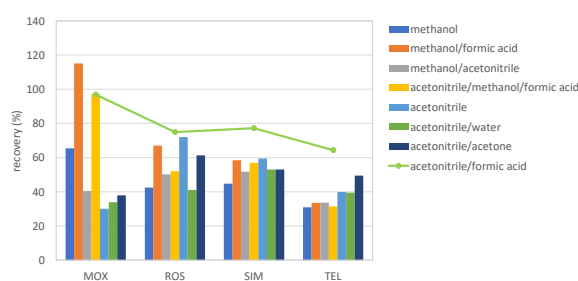
The higher the sorbent mass, the higher the recoveries. This is especially true for very polar MOX.

### 3) Time



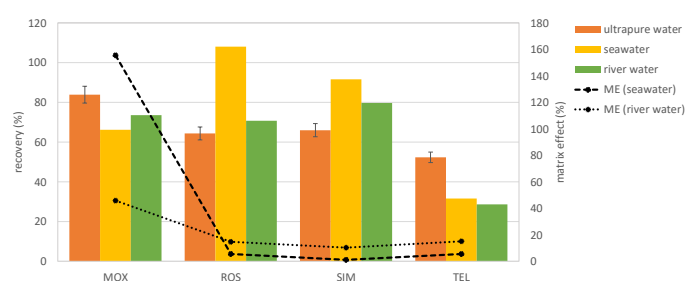
Prolonged extraction (30 min), twitching (30 min), and desorption (30 min) times were the most beneficiary for extraction efficiency. However, in general no significant effects were observed.

### 4) Desorption solvent



Acidic conditions (by adding formic acid) were found the most important parameter in desorption regardless of the solvent. However, acidic acetonitrile finally provided the best compromise of recoveries compared to slightly less efficient acidic methanol.

### 5) Method performance



Optimized method had recoveries between 50 and 80% reaching > 25 preconcentration factors. Recoveries obtained in seawater/river water were different compared to ultrapure water suggesting the impact of the ionic strength. Repeatability was < 5% RSD. Matrix effects were below 20% except for MOX (the most polar & first-eluting analyte) that suffered up to 100% signal enhancement in seawater.

## CONCLUSIONS

DMSPE-HPLC-UV is a promising & simple procedure with high multiplexing capacity. It is applicable for fast extraction & preconcentration of analytes in water analysis.

# ŠTUDIJA DEGRADACIJE ZGODOVINSKEGA PAPIRJA Z METODAMI POSPEŠENE RAZGRADNJE

Nik Nikolić\*, Jan Ocepek†, Ida Kraševac, Matija Strlič

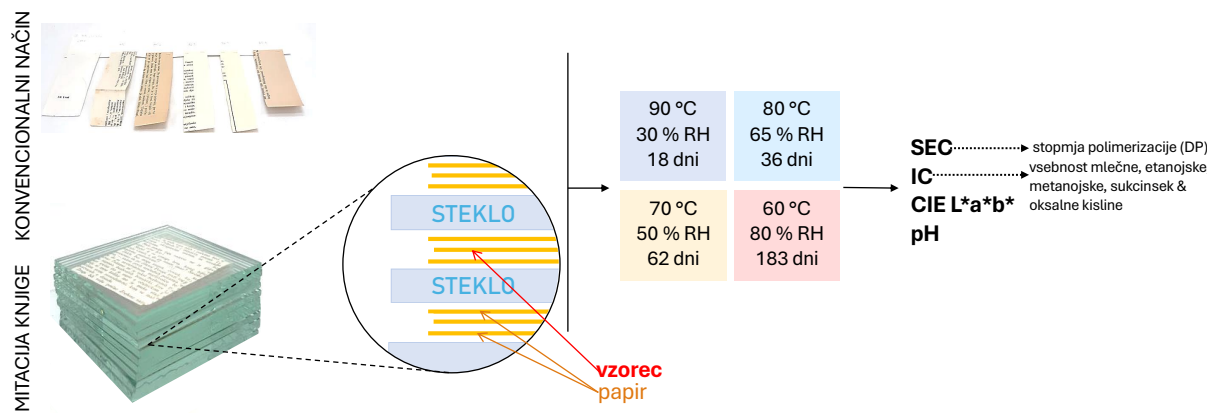
Univerza v Ljubljani, Fakulteta za kemijo in kemijsko tehnologijo

\*nik.nikolic18@gmail.com, †jan.ocepek@gmail.com

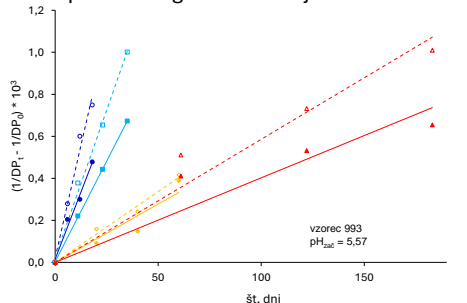
Kislinsko katalizirana hidroliza in oksidacija sta glavna procesa razgradnje papirja. Njune posledice lahko vodijo do izgube knjižne in tiskane dediščine. Med razgradnjo papirja se krajšajo polimerne celulozne verige; oksidacijski produkti povzročijo njegovo rumenjenje; kisli produkti pa znižujejo pH-vrednost papirja.

Spremembe papirja med njegovim staranjem, ki so pri sobnih pogojih nezaznavne, opazujemo z **metodo pospešene razgradnje**, pri kateri vzorce izpostavimo povečani temperaturi in relativni vlažnosti. Na podlagi ekstrapolacije rezultatov na sobne pogoje lahko proučimo dejavnike, ki pospešujejo oz. zavirajo razgradnjo in napovemo, kako se bodo lastnosti papirja spremenjale in življensko dobo papirja.

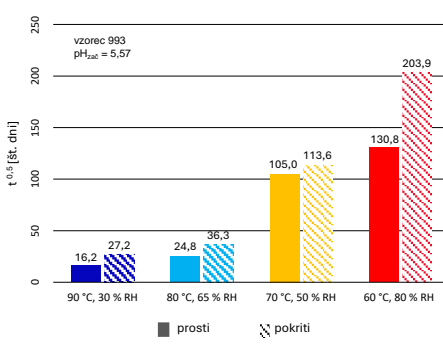
**CILJ RAZISKAVE:** Ovrednotenje vpliva temperature, relativne vlažnosti (RH), lignina in načina razgradnje na degradacijo papirja



Iz sprememb stopenj polimerizacije (DP) med pospešeno razgradnje smo izračunali konstante razgradnje pri posameznih pogojih, iz teh pa nato razpolovni čas razgradnje. Predpostavili smo prvi red razgradnih reakcij.



Graf 1: Vpliv različnih eksperimentalnih pogojev na razgradnjo celuloze v vzorcu 993. Prosti vzorci so označeni s polno črto, pokriti pa s črtkano

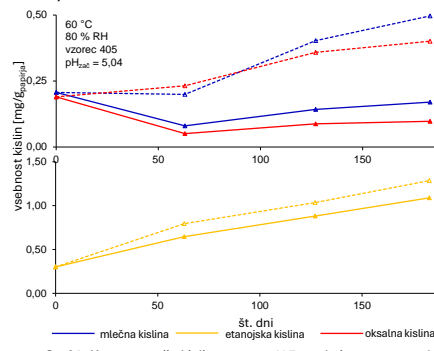


Graf 2: Primerjava  $t^{0.5}$  med pokritimi in prostimi vzorci pri različnih pogojih

Pri vseh pogojih pospešene razgradnje je degradacijski razpolovni čas  $t^{0.5}$  **manjši pri pokritih vzorcih**, kar pomeni, da tam razgradnja poteka hitreje. Razgradnja je najhitrejša pri 90 °C, 30 % RH, najpočasnejsa pa pri 60 °C, 80 % RH.

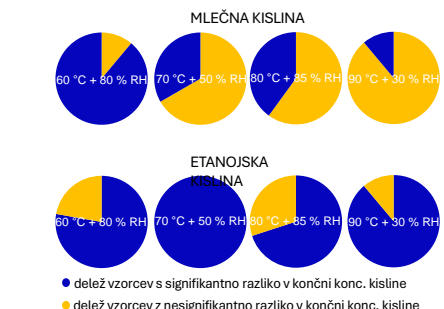
**Pokritim vzorcem se je pH-vrednost med pospešeno razgradnjo znižala bolj kot prostim vzorcem.** Hitrosti spremenjanja pH so višje pri višjih temperaturah pospešene razgradnje.

Vsebnost večine kislin, ki so v vzorcu že prisotne, na začetku pade zaradi njihovega izhlapevanja (metanojska, etanojska kislina) oz. oksidacije (mlečna kislina). Koncentracija oksalne kisline narašča med celotno razgradnjo, predvsem ker je pri pogojih razgradnje končni produkt oksidacije. **Izhlapecanje/oksidacija je izrazitejše pri prostih vzorcih** (polna črta grafa spodaj), akumulacija pa v pokritih (prekinjena črta).



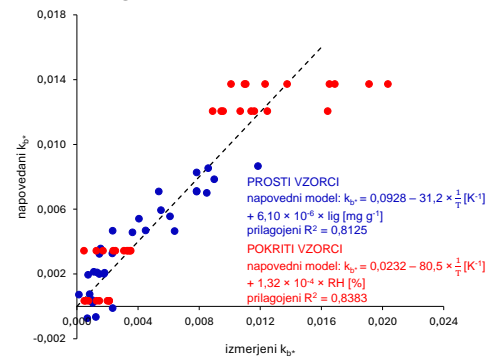
Graf 3: Koncentracija kislin v vzorcu 405 med njegovo razgradnjo

Končne koncentracije merjenih kislin v pokritih vzorcih smo primerjali s Studentovim testom. Razlika med koncentracijo etanojske kisline v pokritih in prostih vzorcih je signifikantna pri večini vzorcev; za mlečno kislino je razlika v koncentraciji signifikantna pri nižjih temperaturah. Pri ostalih kislinah razlike med končnimi koncentracijami v prostih in pokritih vzorcev niso statistično pomembne.



Med razgradno papirja sta se najbolj spremnjeni barvni koordinati  $b^*$  in  $L^*$ . Hitrost rumenjenja smo izračunali kot  $k_{b^*} = \ln(b^*)/t_{\text{razgradnje}}$  in s pomočjo MLR ustarili model, ki napove  $k_{b^*}$ .

**Hitrosti rumenjenja pokritih vzorcev so višje od hitrosti rumenjenja prostih vzorcev.**  $k_b$  je odvisna predvsem od temperature, pri pokritih vzorcih pa tudi od RH in pri prostih vzorcih od vsebnosti lignina.



V nadalnjih raziskavah bomo poskusili merjene lastnosti povezati z vsebnostjo lignina.



# Preučevanje interakcije PD-1/PD-L1 v mikrookolju glioblastoma

Pia Mencin<sup>1,2</sup>, Metka Novak<sup>2</sup>, Barbara Breznik<sup>2</sup>

**NIB** NACIONALNI INSTITUT ZA BIOLOGIJO  
NATIONAL INSTITUTE OF BIOLOGY

<sup>1</sup>Fakulteta za kemijo in kemijsko tehnologijo, Univerza v Ljubljani

<sup>2</sup>Nacionalni inštitut za biologijo

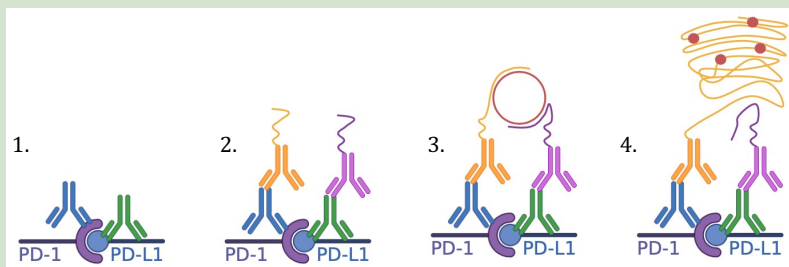
**FKKT**  
UNIVERZA  
V LJUBLJANI  
Fakulteta za kemijo  
in kemijsko tehnologijo

## UVOD

- Glioblastom je najpogosteji primarni maligni tumor osrednjega živčnega sistema, ki velja za neozdravljivega s trenutnimi terapevtskimi pristopi [1].
- Tumorsko mikrookolje glioblastoma je interheterogeno (med bolniki) in intraheterogeno (znotraj posameznega tumorja bolnika), kar otežuje razvoj univerzalno učinkovite terapije [2].
- Potencialne terapevtske tarče so imunske kontrolne točke, kot je tudi inhibitorni receptorski par: receptor programirane celične smrti 1/ligand programirane celične smrti 1 (PD-1/PD-L1) [3].
- Zaradi raznolikosti tumorjev med bolniki uporaba protiteles proti PD-1 in PD-L1 za zdravljenje številnih vrst raka ni uspešna pri vseh bolnikih. Zato je ključnega pomena identificirati bolnike, pri katerih bi bila ta terapija učinkovita.

## METODE

Trenutne študije kot potencialen indikator za uspešnost imunoterapije proti PD-1 in/ali PD-L1 predlagajo samo interakcijo PD-1/PD-L1. Za določitev interakcije smo izbrali metodo test ligacijske bližine (PLA), ki omogoča *in situ* vizualizacijo in kvantifikacijo proteinskih interakcij na molekularnem nivoju. Uporabili smo komplet reagentov Naveni PD1/PD-L1 Atto647N, proizvajalca Navinci.



Zgornja slika prikazuje glavne stopnje metode PLA: 1. inkubacijo s primarnimi protitelesi (Ab) proti tarčnim epitopom, 2. inkubacijo z naveni Ab (sekundarna protitelesa konjugirana z enoverižnim oligonukleotidom), 3. nastanek krožne DNA iz plus in minus oligov naveni Ab in povezovalnih oligov, 4. podvojevanje in detekcija.

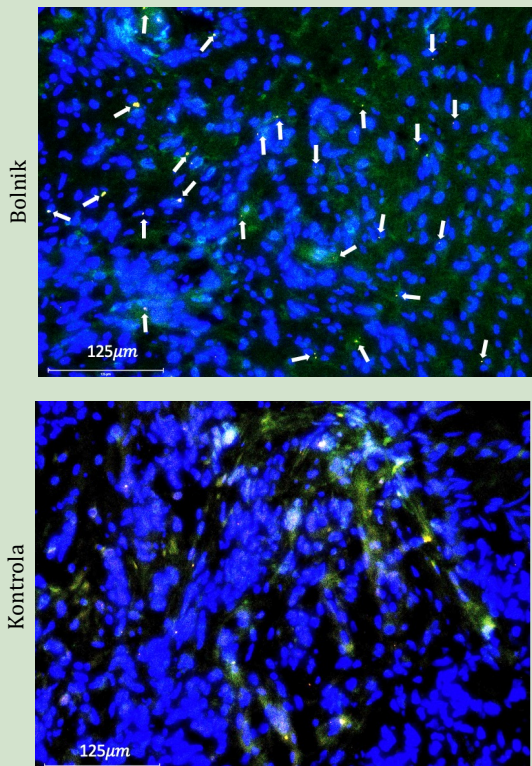
## ZAKLJUČEK

V sklopu diplomske naloge smo potrdili prisotnost interakcije PD-1/PD-L1 v tumorskih biopsijah in organoidih glioblastoma ter primerljivo število interakcij PD-1/PD-L1 v tumorskih biopsijah in organoidih glioblastoma. Pa vendar na podlagi pridobljenih rezultatov ne moremo narediti zagotovih sklepov, saj je eksperimentalno delo zajemalo premajhno število vzorcev in so bili signali negativnih kontrol razmeroma visoki. Kljub temu rezultati predstavljajo obetaven začetek identifikacije metod za določanje primernosti terapij proti PD-1 in PD-L1. Uporaba metode PLA bi bila lahko aplikativna tudi pri zdravljenju ostalih heterogenih tumorjev, ne le glioblastoma.

## REFERENCE

- [1] Q. T. Ostrom, M. Price, C. Neff, G. Cioffi, K. A. Waite, C. Kruchko, J. S. Barnholtz-Sloan: CBTRUS Statistical Report: Primary Brain and Other Central Nervous System Tumors Diagnosed in the United States in 2016–2020. *Neuro Oncol* 2023, 25, iv1–iv99.
- [2] S. DeCordova, A. Shastri, A. G. Tsolaki, H. Yasmin, L. Klein, S. K. Singh, U. Kishore: Molecular Heterogeneity and Immunosuppressive Microenvironment in Glioblastoma. *Front Immunol* 2020, 11, 1402.
- [3] T. Yang, Z. Kong, W. Ma: PD-1/PD-L1 immune checkpoint inhibitors in glioblastoma: clinical studies, challenges and potential. *Hum Vaccin Immunother* 2021, 17, 546.

## REZULTATI



Prisotnost interakcij PD-1/PD-L1 na tkivni rezini biopsije glioblastoma bolnika (zgoraj) in pripadajoča negativna kontrola (spodaj). Na vzorcih je bil izveden PLA, inkubacija s fluorescenčno označenimi protitelesi proti označevalcu levkocitov CD45 ter barvanje jeder s Hoechst. Z belo puščico so označene zaznane interakcije PD-1/PD-L1. Vzorci so bili opazovani s fluorescentnim invertnim mikroskopom pri 200× povečavi, merilo na slikah je 125 μm.

## KONTAKT

piamencin@gmail.com

# Optimization of analytical methods for photodegradation products of PAH and phthalate esters adsorbed on microplastics

Katarina Čubej<sup>1\*</sup>, Samo Bordon<sup>1</sup>, Jena Jamšek<sup>2</sup>, Oliver Bajt<sup>2</sup>, Helena Prosen<sup>1</sup>

<sup>1</sup> Faculty of Chemistry and Chemical technology, University of Ljubljana, Ljubljana, Slovenia

<sup>2</sup> National Institute of Biology – Marine Biology Station Piran, Piran, Slovenia

\* Corresponding author: [katarina.cubej@gmail.com](mailto:katarina.cubej@gmail.com)

Microplastics (MPs) are particles smaller than 5 mm in diameter and present a global environmental pollution problem. MPs serve as vectors for organic pollutants and therefore modify their photodegradation pathways [1]-[3].

The aim of this research was the optimization of analytical methods for photodegradation products adsorbed on MPs for two groups of important environmental pollutants: phthalate esters and polycyclic aromatic hydrocarbons.

## HPLC method

### Standard solutions used

#### PHthalates

phthalic acid (a)

monomethyl phthalate (b)

dimethylphthalate (d)

monobutylphthalate (g)

dibutyl phthalate (k)

#### PAH

2,7-naphthalenediol (c)

acenaphthenequinone (e)

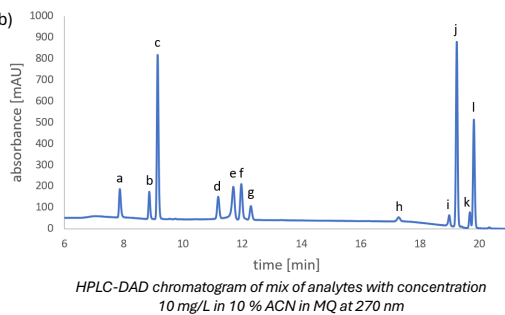
2-naphthol (f)

naphthalene (h)

acenaphthene (i)

phenanthrene (j)

fluoranthene (l)

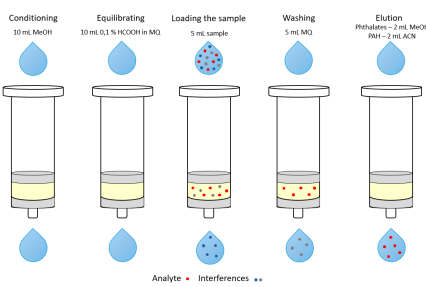


## Solid Phase Extraction

### Optimised for both groups separately

#### Final procedure:

- Column:  
phthalates: HLB  
PAH: LC-8
- pH value of the sample:  
original
- Ion strength of the sample:  
38 ‰ NaCl (sea salinity)  
increases SPE yield\*
- Washing step:  
5 mL MQ
- Elution solvent:  
phthalates: 2 mL MeOH  
PAH: 2 mL ACN

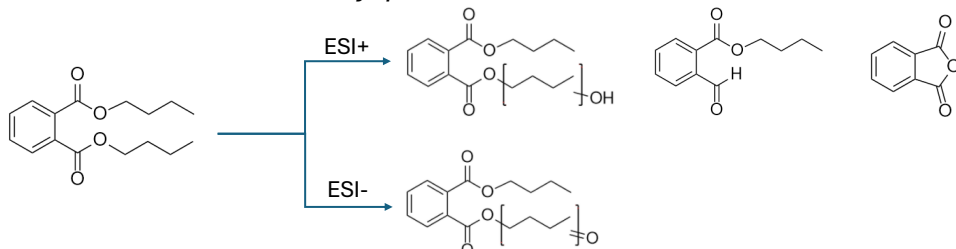


\*did not use it on model samples to avoid formation of adducts

## LC-MS/MS method and TOF MS analysis

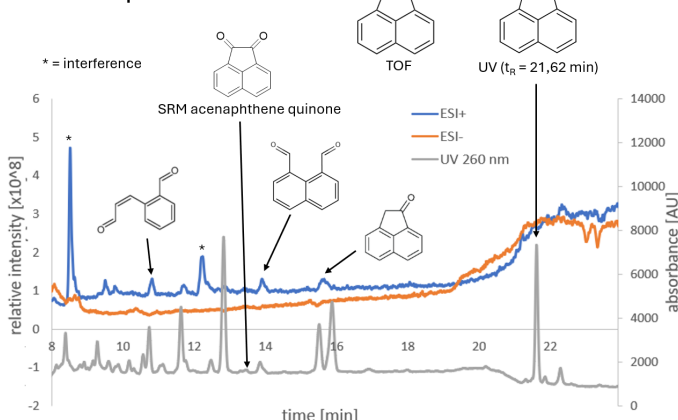
The complete optimised method was applied to model aqueous samples. Identities of peaks were proposed based on fragmentation patterns and confirmed with additional high-resolution MS analysis.

### • Electrooxidation of dibutyl phthalate

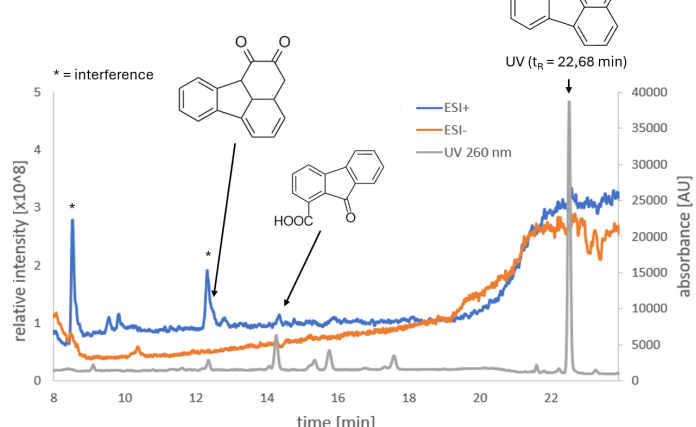


### • Photodegradation of PAH adsorbed on MP's particles

#### Acenaphthene



#### Fluoranthene



## CONCLUSION

With the optimised method, some structures of degradation products of dibutyl phthalate and PAH were successfully determined.

### Reference

- [1] Y. Yu, W. Y. Mo, T. Luukkonen: Adsorption Behaviour and Interaction of Organic Micropollutants with Nano and Microplastics – A Review. *Sci. Total Environ.* **2021**, 797, 149140.
- [2] L. Fu, J. Li, G. Wang, Y. Luan, W. Dai: Adsorption Behavior of Organic Pollutants on Microplastics. *Ecotoxicol. Environ. Saf.* **2021**, 217, 112207.
- [3] J. Huang, P. Duan, L. Tong, W. Zhang: Influence of Polystyrene Microplastics on the Volatilization, Photodegradation and Photoinduced Toxicity of Anthracene and Pyrene in Freshwater and Artificial Seawater. *Sci. Total Environ.* **2022**, 819, 152049.

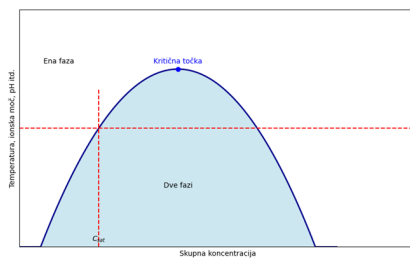
# VPLIV OZNAKE FLAG NA FAZNO SEPARACIJO TEKOČE-TEKOČE

Avtor: Žiga Koren  
Mentor: doc. dr. San Hadži

Ključne besede: fazna separacija tekoče-tekoče, oznaka FLAG, FPLC, UV-Vis, kloniranje s sestavljanjem *in vivo*

## Uvod

Fazna separacija tekoče-tekoče (LLPS) je način fazne separacije, v katerem raztopine makromolekul, na primer proteinov ali nukleinskih kislin, kondenzirajo v bolj gosto tekoče fazno stanje, podobno kapljam. Bolj kondenzirana faza soobstaja z redkejšo fazo. Do LLPS pride zaradi intramolekularnih sil, kot so kation-anion, dipol-dipol,  $\pi$ - $\pi$  in kation- $\pi$  interakcije. Nastanek kondenzatov je odvisen od koncentracije makromolekula ter od zunanjih dejavnikov. Odvisno od teh dveh parametrov se makromolekula lahko nahaja v eni ali v dveh fazah. LLPS je v celicah ključen za tvorbo brezmembranskih organelov, pospeševanje biokemijskih reakcij in za varovanje celic pred variacijami v koncentracijah makromolekul, saj so koncentracije znotraj faz konstantne, menjuje se le volumski delež med njimi.

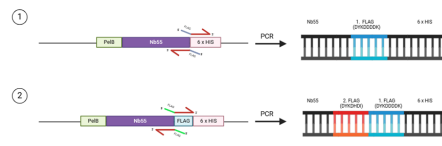


## Namen

Tvorba kondenzatov z LLPS lahko vpliva na fizikalne lastnosti in na funkcijo proteina. Sintetični epitop FLAG je pogosto uporabljen fuzijski partner. Zanimalo nas je, če dodatek oznake FLAG vzpodbudi tvorbo LLPS, saj lahko fenomen predstavlja potencialen vpliv na druge raziskave.

## Metode

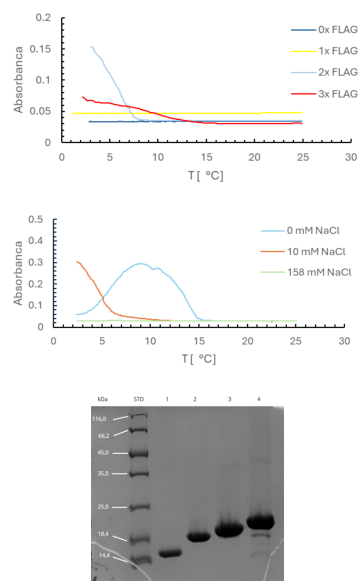
Pripravili smo konstrukte preiskovanega proteina (nanotelesa 55) z 0x, 1x, 2x in 3x oznako FLAG z uporabo kloniranja s sestavljanjem *in vivo* (IVA). Proteine smo izolirali s kovinsko-kelatno imobilizirano kromatografijo (IMAC), pojavu smo sledili z UV-Vis spektrofotometrom pri 550 nm s hlajenjem s hitrostjo 0,1 °C/min.



## Rezultati in diskusija

Rezultate izolacije rekombinantnih proteinov, pridobljenih s kloniranjem IVA, smo preverili s poliakrilamidno gelsko elektroforezo z natrijevim dodecil sulfatom. Proteini so se med seboj razlikovali v zapisu za 1x FLAG (DYKDDDDK), pričakovali smo razlike okoli 1 kDa, kar se tudi sklada s pridobljenimi rezultati. Ob hlajenju smo pojav LLPS zaznali kot porast absorbance, do katerega pride zaradi sisanja svetlobe po pojavu goste faze. Vzorec 3x FLAG je tvoril kondenzate pri temperaturi 13 °C, vzorec 2x FLAG pa pri 8 °C. Pri vzorcih 1x FLAG in 0x FLAG do pojava ni prišlo, kar ponazarja pomembnost prisotnosti intramolekularnih sil, ki jih omogoča oznaka FLAG, za tvorbo kondenzatov. Pojav smo spremljali tudi pri naraščajoči koncentraciji NaCl, pri čemer smo ugotovili, da nizke koncentracije soli zavirajo, višje pa popolnoma zatrejo LLPS.

Z eksperimenti smo pokazali, da prisotnost oznake FLAG poveča nagnjenost proteina k temu, da tvori biomolekularne kondenzate. Kondenzati vplivajo na različne biokemijske lastnosti makromolekul, ki jih tvorijo. Lokalno koncentrirani encimi hitreje vršijo biokemijske reakcije kot tisti, ki se ne nahajajo v kondenzatih, saj so kondenzati dinamične strukture, ki omogočajo hitrejšo izmenjavo snovi. Proteini v kondenzatih lahko tudi zavirajo biokemijske reakcije, saj služijo kot fizične ovire, ali pa se zaradi LLPS narobe zvijejo, kar ovira njihovo funkcijo. Glede na uporabnost oznake FLAG pri detekciji in izolaciji proteinov, je pomembno, da se pred raziskavami, posebej pri raziskavah kinetičnih lastnosti encimov, preveri, če do pojava pride, saj lahko zaradi LLPS pride do nesklaanja med rezultati *in vitro* in med dogajanjem *in vivo*.



## Zaključek

Uspešno smo pripravili in izrazili proteinske produkte in potrdili povezavo med številom ponovitev oznake FLAG in med tvorbo LLPS. V prihodnjih raziskavah bi bilo dobro pripraviti samostojen polipeptid FLAG in preveriti, če tvori LLPS. Sam pojav je viden na makroskopski ravni, kar v prihodnje omogoča tudi slikanje kondenzatov pod mikroskopom. Ugotovili smo tudi, da prisotnost soli zavira pojav, kar bi lahko pri pomoglo k preprečevanju pojava pri raziskavah, kjer LLPS bistveno spremeni lastnosti obravnavanega proteina.

## Reference

- Z. Gao, W. Zhang, R. Chang, S. Zhang, G. Yang, G. Zhao: Liquid-Liquid Phase Separation: Unraveling the Enigma of Biomolecular Condensates in Microbial Cells. *Front. Microbiol.* 2021, 12, 751800.  
S. Alberti, A. Gladfelter, T. Mittag: Considerations and Challenges in Studying Liquid-Liquid Phase Separation and Biomolecular Condensates. *Cell* 2019, 176, 419–434.  
W. Li, C. Jiang, E. Zhang: Advances in the phase separation-organized membraneless organelles in cells: a narrative review. *Transl Cancer Res* 2021, 10, 4929–4946.

Tadeja Kuret<sup>1</sup>, Janja Bohte<sup>2</sup>, Peter Veranič<sup>1\*</sup>

<sup>1</sup>Institute of Cell Biology, Faculty of Medicine, University of Ljubljana <sup>2</sup>Faculty of Chemistry and Chemical Technology, University of Ljubljana

## INTRODUCTION & AIM

**Interstitial cystitis** is a chronic inflammatory disease of the urinary bladder with no long-term effective treatment available to date.

The exact etiology and pathobiology of the disease remain unknown, however, **disturbed assembly of urothelial cell tight junctions, increased urine-blood barrier permeability, inflammation and oxidative stress** have been proposed to play crucial roles.

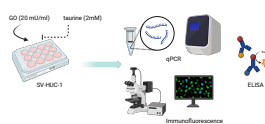
Agents that can simultaneously modulate all processes associated with interstitial cystitis will be of paramount importance for future therapy.

One such example is **taurine** (2-aminoethanesulfonic acid), the most abundant free amino acid in human. Taurine has already been shown to reduce inflammation as well as oxidative stress and improve integrity of various epithelial tissues.

Our aim was to look into the effects of taurine on inflammation, oxidative stress and blood-urine barrier function of urothelial cells in an *in vitro* model of interstitial cystitis.

## METHODS

The *in vitro* model consisted of normal human urothelial cell line SV-HUC1, stimulated with glucose oxidase (GO; 20 mM/ml), which mimics prolonged low levels of oxidative stress. Cells were preincubated with taurine (2 mM) for 2h and then stimulated with/without GO for 24h. Untreated cells served as control. Cells were lysed for RNA isolation and subsequent qPCR analysis while protein levels were determined by ELISA and immunofluorescence (IF).

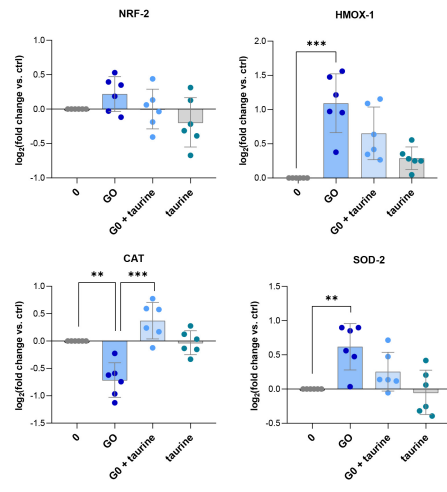


## CONCLUSION

Our findings suggest that taurine has the potential to mitigate inflammation, oxidative stress as well as maintain the integrity of the urothelial barrier, all of which are implicated in the development and progression of interstitial cystitis.

## Taurine upregulates catalase

Taurine upregulated the mRNA expression of the antioxidant enzyme catalase (CAT), downregulated by stimulation with GO. However, no influence of taurine on the expression of the redox sensitive transcription factor NRF-2 and the antioxidant enzymes SOD-2 and HMOX-1 were observed.



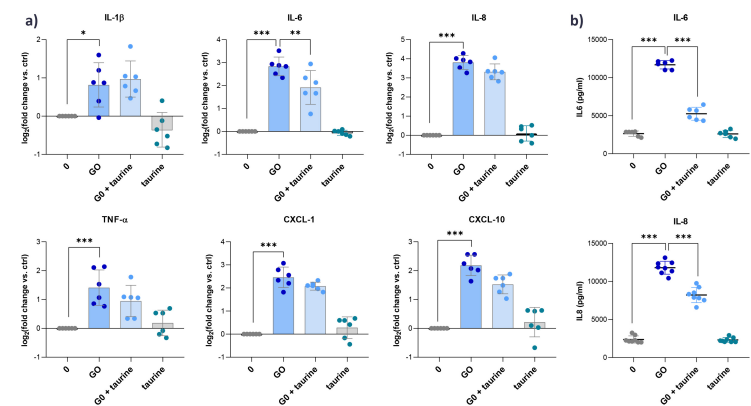
**Effects of taurine on NRF2-activation pathway and antioxidant enzymes in GO-stimulated cells**, determined by the qPCR method, normalized to the endogenous controls ACTB and GAPDH. Shown are means  $\pm$  SD for each group.

\*\*p<0.01; \*\*\*p<0.001.

## RESULTS

### Taurine downregulates oxidative stress-induced inflammatory mediators

Taurine significantly downregulated the mRNA expression of the inflammatory cytokine IL-6, and the chemokines CXCL-1, and CXCL-10, which were upregulated by stimulation with GO. No significant effect of taurine was observed on the mRNA expression of IL-1 $\beta$  and TNF- $\alpha$ . The protein levels of IL-6 and IL-8 released in the supernatants of urothelial cells incubated with taurine were also significantly lower compared to cells stimulated with GO.

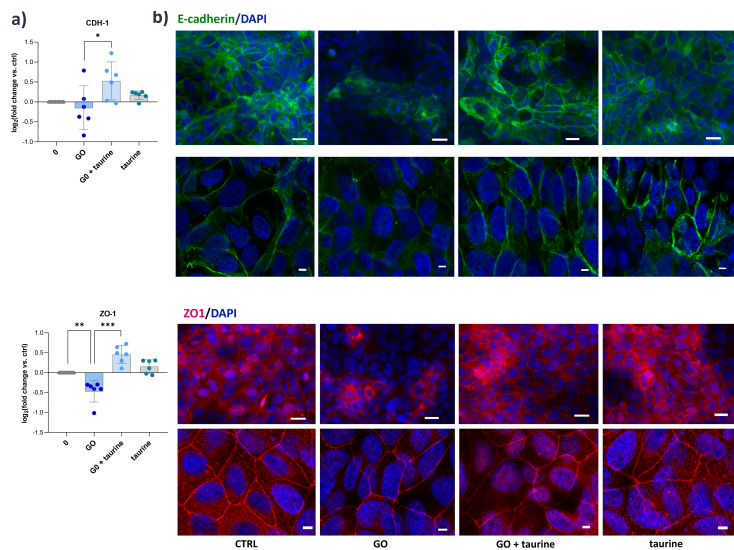


**Effects of taurine on inflammatory mediators in GO-stimulated cells.** a) mRNA expression of inflammatory cytokines and chemokines, obtained by the qPCR method, normalized to the endogenous controls ACTB and GAPDH. b) protein levels of IL-6 and IL-8, determined by ELISA. Shown are means  $\pm$  SD for each group.

\*p<0.05; \*\*p<0.01; \*\*\*p<0.001.

### Taurine reverses the assembly of intercellular contacts disrupted by oxidative stress

Taurine significantly increased the mRNA expression of E-cadherin, encoding for adherent junction protein and zonula occludens-1 (ZO-1), encoding tight junction protein, which were downregulated in the presence of GO. This was subsequently confirmed also on protein levels showing altered assembly of adherens and tight junctions in the presence of GO, reversed by the addition of taurine.



**Effects of taurine on intercellular junctions in GO-stimulated cells.** a) mRNA expression of CDH-1 and ZO-1, obtained by the qPCR method, normalized to the endogenous controls ACTB and GAPDH. Shown are means  $\pm$  SD for each group. \*p<0.05; \*\*p<0.01; \*\*\*p<0.001. b) Representative images showing localization and distribution of E-cadherin (green) and ZO-1 (red). Nuclei are stained blue. Images were taken at the 20x and 63x magnification. Scale bars: 20  $\mu$ m and 5  $\mu$ m.

# Nepričakovan preobrat pri inhibiciji invazije rakavih celic!

5% petletno preživetje

300.000 novih primerov na leto na svetu

AVTOR: Ula Mikoš

## Namen

**Glioblastom** je primarni možganski tumor, ki je eno najbolj agresivnih in smrtonosnih malignih obolenj. Njegova agresivnost se kaže v hitri difuzni invaziji, ki vodi do visoke stopnje ponovitve in na koncu do slabe prognoze.

**CD155** (imenovan tudi kot PVR ali Necl-5) se v rakavih celicah izraža v povečani meri, kar je povezano z agresivnostjo tumorja. Zaradi njegove vloge pri regulaciji celične adhezije in migracije je CD155 potencialna tarča za zdravljenje glioblastoma.

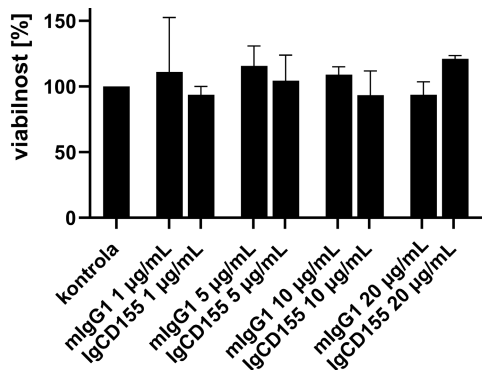
**Namen** diplomskega dela je bil raziskati vlogo proteina CD155 pri rasti in invaziji celic glioblastoma. Zanimalo nas je, ali lahko z uporabo protitelesa proti CD155 vplivamo na invazivnost celic glioblastoma in s tem potencialno izboljšamo možnost za zdravljenje.

## Metode

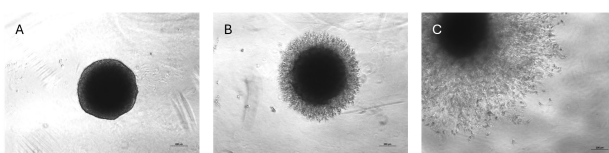
- Gojenje celic **NIB140** (glioblastomska celična linija vzpostavljena na NIB).
- **MTT test celične viabilnosti** (koncentracije 1 µg/mL, 5 µg/mL, 10 µg/mL in 20 µg/mL protitelesa proti CD155 (IgCD155) in mišjega kontrolnega protitelesa IgG izotipa 1 (mIgG1)). S tem testom smo želeli ugotoviti ali ima protitelo toksičen učinek na celice glioblastoma.
- **3D test invazije sferoidov v Matrigelu** (tretiranje s koncentracijo 10 µg/mL). S tem testom smo simulirali invazijo celic glioblastoma v 3D prostoru. Opazovali smo, kako protitelo vpliva na sposobnost celic, da se širijo v umetni zunajcelični matriks (Matrigel).
- **Analiza invazije s programom ImageJ.**

## REZULTATI

### IgCD155 ne vpliva na viabilnost celic NIB140

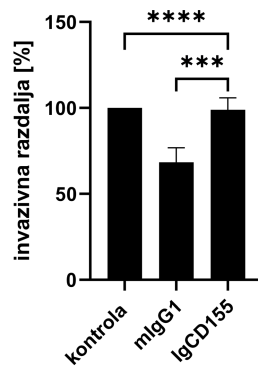


Slika 1: Viabilnost celic NIB140 48 h po tretirjanju z različnimi koncentracijami IgCD155 in mIgG1. Prikazane so povprečne viabilnosti in standardni odklon. Kontrolo predstavljajo celice v dopolnjenem gojišču, brez dodatka protiteles.

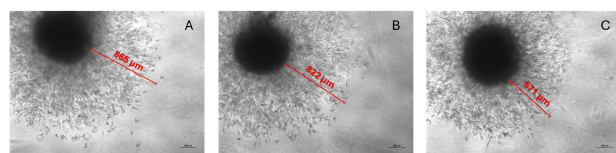


Slika 2: Primerjava invazije celic sferoida NIB140 v času inkubacije brez dodatka protiteles. A – sferoid v začetnem stanju, B – sferoid po 24 h inkubacije, C – sferoid po 96 h inkubacije.

### IgCD155 ne vpliva na invazijo celic NIB140 mIgG1 zmanjša invazijo za 30 – 40 %



Slika 3: Invazivna razdalja celic sferoidov NIB140 96 h po tretmaju z IgCD155 in mIgG1. Prikazane so povprečne invazivne razdalje in standardni odklon. Kontrolo predstavljajo celice v dopolnjenem gojišču, brez dodatka protiteles. Legenda: \*\*\* = p < 0,001 in \*\*\*\* = p < 0,0001.



Slika 4: Invazija celic sferoida NIB140 96 h po tretmaju. A – kontrola brez protitelesa, B – z dodatkom IgCD155, C – z dodatkom mIgG1.

## Razprava

Protitelo proti CD155 ni vplivalo na invazijo celic glioblastoma, vendar ne moremo z gotovostjo trditi, da IgCD155 ne inhibira invazije celic glioblastoma, saj bi poskus morali ponoviti na večjem številu glioblastomskih celičnih linij, prav tako bi morali testirati še druge koncentracije protitelesa. Za najbolj realno sliko, kako protitelo vpliva na tumor, pa bi morali uporabiti celične modele kot so glioblastomski organoidi.

**Mišje kontrolno protitelo IgG izotipa 1 je zmanjšalo invazijo celic glioblastoma**, kar je verjetno posledica njegove vezave na Fc receptorje in ne neposrednega toksičnega učinka protitelesa, saj smo uporabili dokazano netoksično koncentracijo protitelesa za našo celično linijo. V pregledani literaturi nismo zasledili, da bi o vplivu mIgG1 na invazijo že kdo poročal, zato je potreben podrobnejši vpogled v delovanje tega protitelesa na invazijo celic glioblastoma, predno lahko predpostavimo njegovo klinično uporabnost.

# Impact of Substrate on Optical Properties of 1-D Photonic Crystals for White LEDs

Martin Jazbec,<sup>1,2</sup> Prasenjit P Sukul,<sup>2</sup> Luís F. Santos,<sup>2</sup> Rui M. Almeida<sup>2</sup>

<sup>1</sup> Faculty of Chemistry and Chemical Technology, University of Ljubljana,  
Večna pot 113, 1000 Ljubljana, Slovenia

<sup>2</sup> Instituto Superior Técnico, University of Lisbon, Av. Rovisco Pais 1,  
1049-001 Lisboa, Portugal

## INTRODUCTION

White light generation (WLG) was achieved by using 1D photonic crystal structures (Bragg mirrors (BM) and Fabry-Pérot microcavities (MC)) on different substrates. Samples with tunable light emission spectra were created by exposing them to different laser light angles, optimizing emission characteristics.

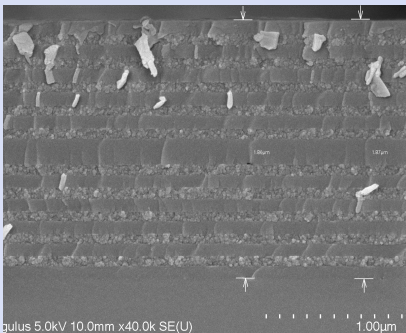


Figure 1: SEM image of MC structure

## MATERIALS & METHODS

### ➤ Sol-gel process:

- High refractive index solution = Titania sol
- Low refractive index solution = Aluminosilicate sol with 0.3/0.5/5.0 mol. % of (Tm<sup>3+</sup>/Er<sup>3+</sup>/Yb<sup>3+</sup>) doping materials

### ➤ Substrates:

- p-type Silicon (100) wafer, SiO<sub>2</sub> (vitreous silica) wafer, Gallium arsenide (GaAs)
- Substrate material significantly impacted the adhesion and optical properties of the deposited layers, affecting light emission spectra.

### ➤ Spin Coating was used for the deposition of thin layers

### ➤ Characterization techniques:

- Ellipsometry, FTIR, SEM, Photoluminescence (PL), Reflectivity

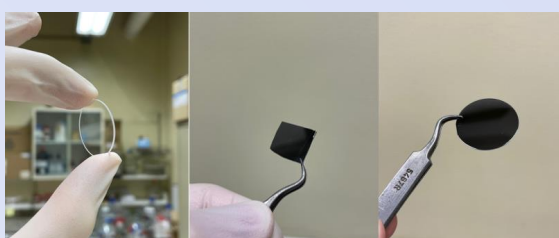


Figure 2: Substrates before deposition; from left to right:  
a) SiO<sub>2</sub> wafer, b) Silicon wafer, c) GaAs, d) MC deposition on Silicon substrate

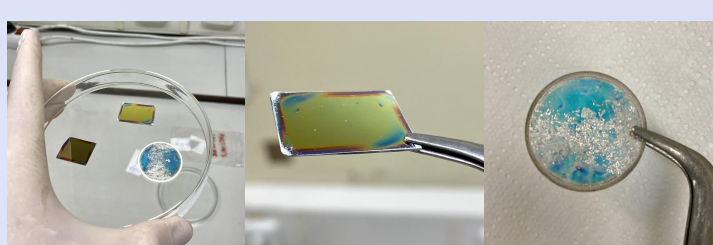


Figure 3: Substrates after deposition; from left to right:  
a) Deposited samples on different substrates, b) MC deposition on Silicon substrate,  
c) BM deposition on Silica substrate

## RESULTS

### ➤ Calibration curves presenting layer thickness as a function of ethanol volume

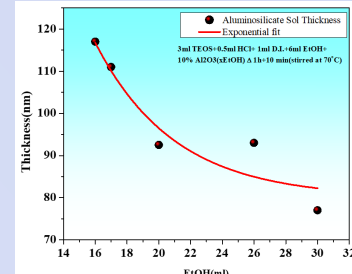


Figure 4: Aluminosilicate sol, layer thickness calibration

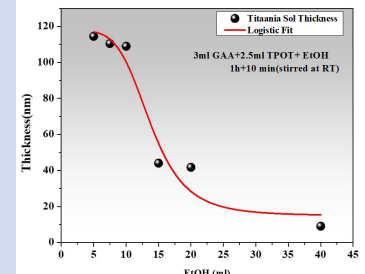


Figure 5: Titania sol, layer thickness calibration

### ➤ Reflectivity measurements (on SiO<sub>2</sub> substrate):

- Lower angle → red emission spectra
- Higher angle → blue emission spectra

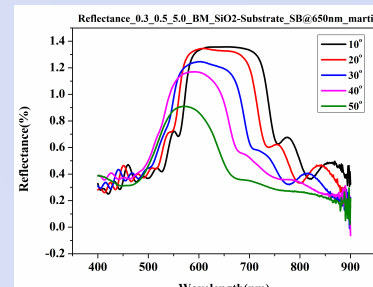


Figure 6: Reflectivity measurements of BM structure on SiO<sub>2</sub> substrate

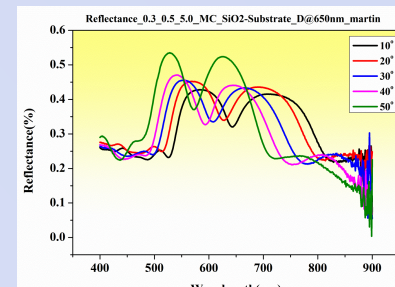


Figure 7: Reflectivity measurements of MC structure on SiO<sub>2</sub> substrate

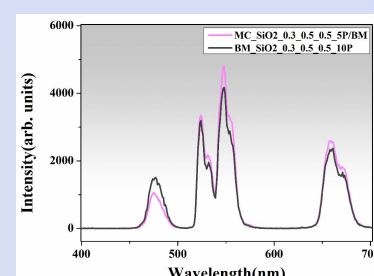


Figure 8: PL spectra of BM and MC structures on SiO<sub>2</sub> substrate

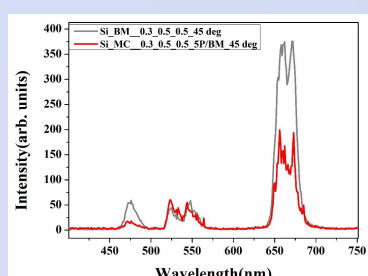


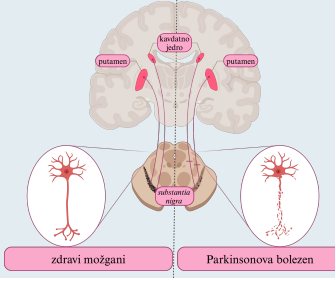
Figure 9: PL spectra of BM and MC structures on Si substrate

## CONCLUSION

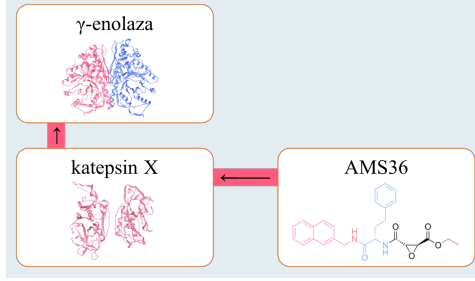
SiO<sub>2</sub> substrate demonstrated superior performance among all three studied substrates, providing the most intense photoluminescence (PL) spectra and peak values at reflectivity measurements within the white light range. Lower angles of laser exposure resulted in red-shifted emission spectra, while higher angles produced more blue-shifted emissions. GaAs was excluded from further research due to poor thermal stability and reactivity with deposited layers during heat treatment.

# Izražanje $\gamma$ -enolaze in njeni uravnavanje s katepsinom X v poškodovanih dopaminergičnih nevroblastomskih celicah SH-SY5Y

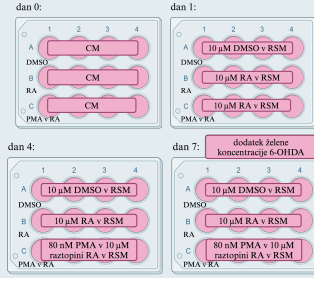
## NEVRODEGENERACIJA PRI PARKINSONOVİ BOLEZNI



## NEVROTROFIČNA PODPORA



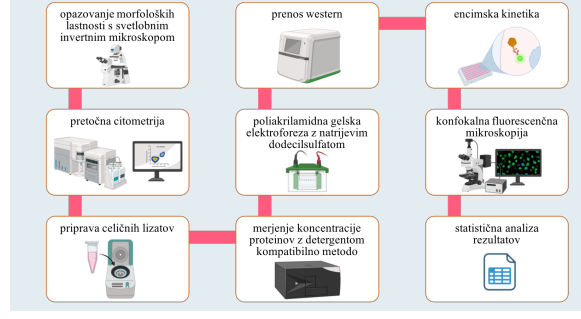
## IN VITRO PROUČEVANJE NEVRODEGENERACIJE



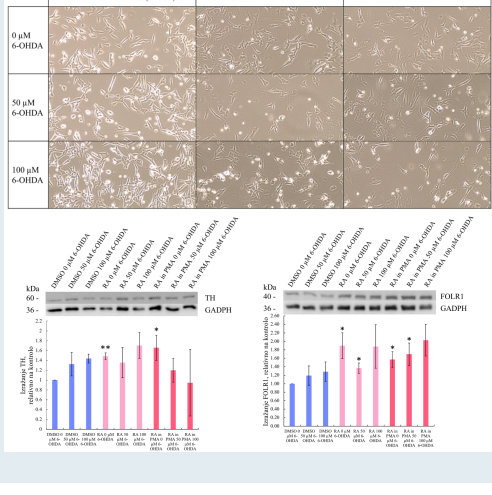
## NAMEN DELA

1. Vzpostavitev modela diferenciacije celic SH-SY5Y
2. Vzpostavitev modela nevrodegeneracije dopaminergičnega podtipa
3. Vrednotenje izražanja  $\gamma$ -enolaze in njene ko-lokalizacije s katepsinom X
4. Vrednotenje zaščitnega vpliva zaviralca katepsina X AMS36

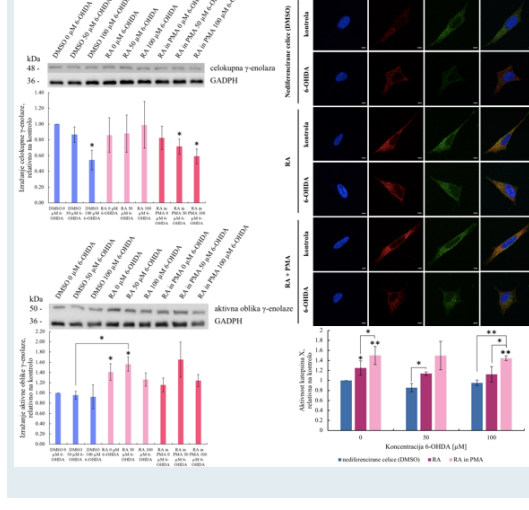
## METODE



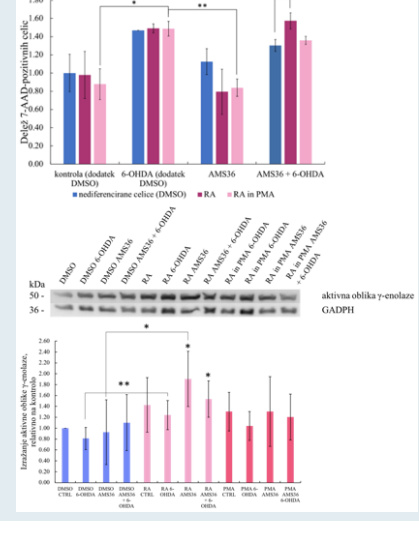
## 1. VZPOSTAVITEV MODELA DIFERENCIACIJE IN NEVRODEGENERACIJE SH-SY5Y



## 2. VREDNOTENJE IZRAŽANJA $\gamma$ -ENOLAZE IN NJENE KO-LOKALIZACIJE S KATEPSINOM X



## 3. VREDNOTENJE ZAŠČITNEGA VPLIVA ZAVIRALCA KATEPSINA X AMS36



## SKLEPI

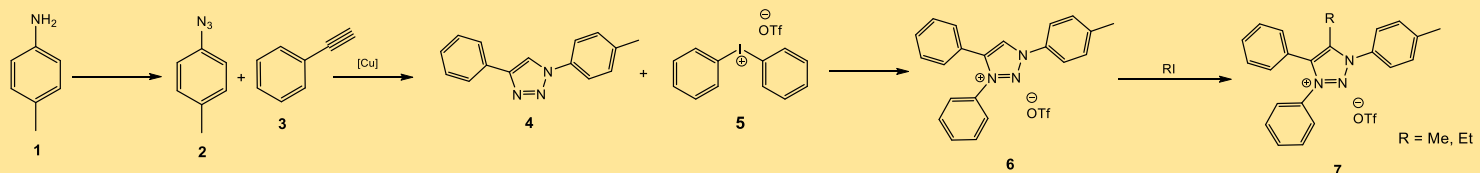
1. Celice SH-SY5Y lahko diferenciramo v dopaminergično podvrsto z dodatkom RA v kombinaciji s PMA, kar se odraža v povišanem izražanju dopaminergičnih označevalcev TH in FOLR1 ter v podaljšanju celičnih izrastkov.
2. Dodatek 6-OHDA poveča delež mrtvih nediferenciranih in diferenciranih celic SH-SY5Y. Za *in vitro* celični model Parkinsonove bolezni je najprimernejša 24-urna vzpostavitev 6-OHDA s končno koncentracijo 50 ali 100  $\mu$ M.
3. Raven izražanja aktivne oblike  $\gamma$ -enolaze je višja pri diferenciranih celicah, raven izražanja celokupne  $\gamma$ -enolaze pa je podobna pri nediferenciranih in diferenciranih celicah. Opazna je ko-lokalizacija  $\gamma$ -enolaze s katepsinom X, ki je izrazitejša v diferenciranih celicah, medtem ko izpostavitev celic 6-OHDA vpliva na zmanjšano ko-lokalizacijo.
4. Aktivnost katepsina X je višja v diferenciranih celicah, pri čemer je najvišja v celicah, izpostavljenih RA in PMA.
5. Dodatek zaviralca katepsina X AMS36 ima zaščitni učinek na nevrotoksične učinke 6-OHDA. Zaviranje katepsina X v celicah, poškodovanih s 6-OHDA, povlači raven izražanja aktivne oblike  $\gamma$ -enolaze.

# Triazolijkeve soli kot napredni ligandi:

## Sinteza in njihova uporabnost



**POVZETEK:** Sintetizirali smo **3,4-difenil-5-metil-1-(*p*-tolil)-1*H*-1,2,3-triazolijev triflat** in **3,4-difenil-5-ethyl-1-(*p*-tolil)-1*H*-1,2,3-triazolijev triflat**. Sintezo smo začeli s 4-aminotoluenom **1**, ki smo ga pretvorili v 4-azidotoluen **2**. Med njim in fenilacetilenom **3** smo izvedli z bakrom katalizirano azid-alkin cikloadicijo (CuAAC) in dobili 1,4-disubstituiran-1,2,3-triazol **4**. Tega smo reagirali z jodonijevo soljo **5** v prisotnosti bakrovega sulfata in dobili 1,3,4-trisubstituirano 1,2,3-triazolijkevo sol **6**. V zadnji stopnji smo na mesto **5**, v prisotnosti reagentov *n*-butillitija in ustreznega alkil jodida vezali metilno ali etilno skupino ter dobili produkta **7**. Ta sta uporabljeni kot liganda, ki ob vezavi kovinskega iona delujeta kot katalizatorja. Karakteritirali smo ju z  $^1\text{H}$ ,  $^{13}\text{C}$  NMR in IR spektroskopijo ter masno spektrometrijo visoke ločljivosti.



### Metodologija

#### Tvorba 1,2,3-triazola z CuAAC:

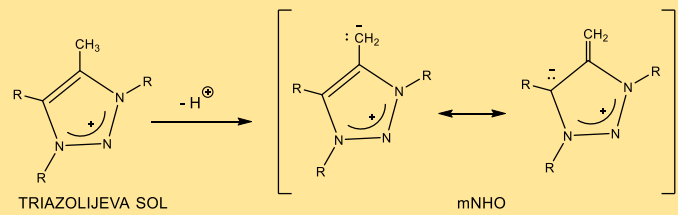
- spada med "klik reakcije", za katere je bila leta 2022 podeljena Nobelova nagrada;
- preprosta in hitra izvedba** brez topila, v prisotnosti katalizatorja  $\text{Cu}(\text{PPh}_3)_3\text{Br}$ , z enostavnim čiščenjem (prekristalizacija);
- povprečen **izkoristek** petih ponovitev je **91 %**.

#### Čiščenje produktov:

- ekstrakcija;
- prekristalizacija;
- kolonska kromatografija;
- filtracija skozi čep silikagela.

### Uporaba triazolijevih soli

Triazolijkeve soli služijo kot prekurzorji za sintezo N-heterocikličnih olefinov (mNHO).



Uporabni so:

- kot **katalizatorji** za reakcije hidroboriranja in N-metiliranja primarnih aminov;
- za **reakcije z Lewisovimi kislinami, kisikom in aril azidi**;
- za **dostop do diazoolefinov** in njihovih ustreznih bakrovih kompleksov.



# Pretvorbe elektronsko bogatih aromatov pri alternativnih pogojih

Skeniraj  
me!



Diplomska delo

Zoja Žnidarič

Mentor: prof. dr. Marjan Jereb

zoja.znidaric@gmail.com

## POVZETEK

V svojem diplomskem delu sem testirala pretvorbo elektronsko bogatih aromatov s karboksilnimi anhidridi in trifluoroacetno kislino (TFA).

Reakcija je trajnostna alternativa klasični reakciji Friedel-Craftsovega aciliranja, saj omogoča sintezo brez uporabe toksičnega in nevarnega katalizatorja  $\text{AlCl}_3$ .

TFA deluje kot katalizator in topilo hkrati, prav tako pa jo lahko po reakciji ponovno uporabimo in se tako izognemo nepotrebnemu odpadku. Aciliranje sem izvajala na spojinah z različno sterično zahtevnimi funkcionalnimi skupinami. Raziskovala sem tudi vpliv strukture elektronsko revnejših oziroma elektronsko bogatejših aromatov na potek aciliranja aromatskega obroča.

## METODOLOGIJA

- Mešanje na sobni temperaturi
- Prekinitve reakcije z dodatkom  $\text{NaHCO}_3$
- Ekstrakcija in odstranitev topila
- Analiza z  $^1\text{H}$  NMR spektroskopijo
- Čiščenje: prekristalizacija, kolonska kromatografija
- Potrditev strukture s HRMS in IR spektroskopijo

Tabela 1: Primerjava TFA in  $\text{AlCl}_3$

Lastnost	TFA	$\text{AlCl}_3$
Vloga	Katalizator in topilo	Katalizator
Nevarnost	Korozivna, vendar manj nevarni stranski produkti	Zelo koroziven, hitro reagira z vlogo do $\text{HCl}$
Okojški vpliv in recikliranje	Možnost recikliranja z destilacijo; manj odpadkov	Težko recikliramo zaradi hidrolize; več odpadkov
Uporaba v sintezi	Primerna za zeleno kemijo	Pogosta v klasičnih sintezah

## REZULTATI

Tabela 2: Pregled produktov

Strukturna formula	Izkoristek [%]
	74,93 %
	92,02 %
	77,14 %
	65,55 %
	91,29 %
	45,05 %
	81,29 %
	2,72 %
	82,56 %
	13,38 %

## ZAKLJUČEK

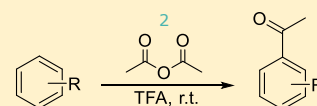
Aciliranje je bilo uspešno na manj sterično zahtevnih spojinah. Izkoristki so bili dokaj visoki, med 50 in 90 %.

Za manj uspešno se je izkazalo na spojinah, ki vsebujejo estrsko funkcionalno skupino. Čeprav lahko estrska skupina, vezana preko kisika, donira elektrone, je resonančni učinek omejen zaradi elektron-privilačnega učinka karbonilne skupine. Tako se posledično zmanjša tudi aktiviranost aromata.

Temeljna literatura: G. Liu, B. Xu: Hydrogen bond donor solvents enabled metal and halogen-free Friedel-Crafts acylations with virtually no waste stream. *Tetrahedron Lett.* 2018, 59, 869-872.

= število ekvivalentov

## PRVI TIP REAKCIJE



Na aromatskih spojinah z acetanhidridom v prisotnosti TFA

## DRUGI TIP REAKCIJE



Na benzojski kislini z 1,3-dimetoksibenzenom v prisotnosti trifluoroacetanhidrida (TFAA) in TFA

# The effect of *Staphylococcus capitis* growth rate on the effectiveness of bacteriophage K

Špela Blaznik, Ana Lisac, Aleš Podgornik

Faculty of chemistry and chemical technology, Ljubljana, Slovenia

## INTRODUCTION

Phage parameters are key for optimizing bacteriophage production and evaluating phage therapy. The **adsorption constant ( $k_a$  [mL/(CFU·h)]**) quantifies phage attachment to bacteria, based on the decline in phage concentration over time. The **latent period (LP) [h]** is the time from infection to lysis, while the **burst size (BS)** measures viruses released per cell. These values depend on the host's physiological state, regulated by adjusting the dilution rate in a chemostat. Bacteriophage replication, relies on this state, utilizing the host's metabolism and components [1, 2]. To prevent bacterial washout, the dilution rate  $D$  [h<sup>-1</sup>] must not exceed the maximum growth rate  $\mu_{\max}$  [h<sup>-1</sup>] [3].

## METHOD

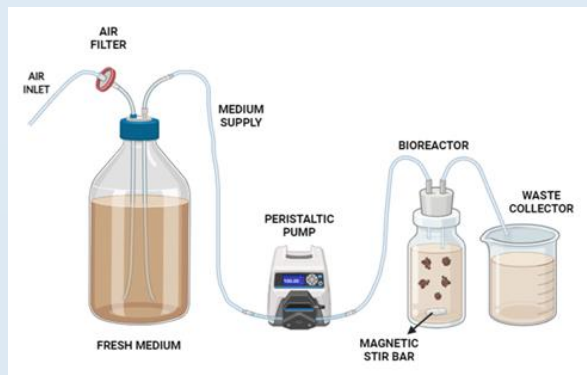


Figure 1: A schematic representation of a chemostat, which enables stationary growth of microorganisms by regulating the inflow of medium.

## RESULTS AND DISCUSSION

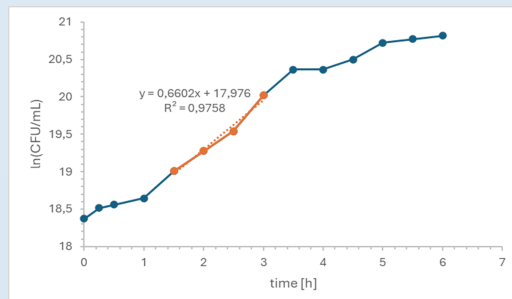


Figure 2: *S. capitis* growth curve with determination of  $\mu_{\max}$

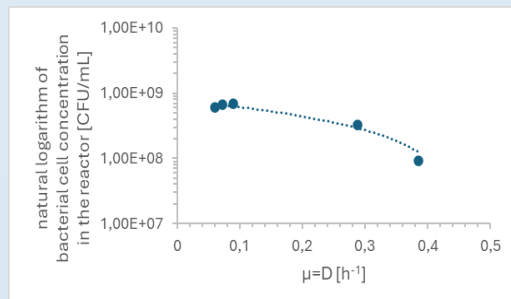


Figure 3: Physiological state of the bacterial culture at different dilution rates

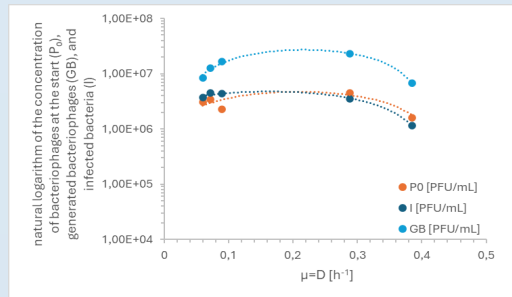


Figure 4: Equilibrium concentration of initial phage concentration, generated bacteriophages and infected bacteria

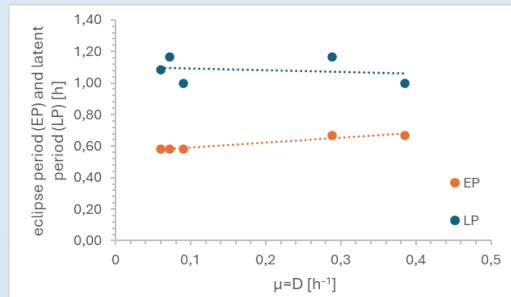


Figure 5: Eclipse and latent period during phage production

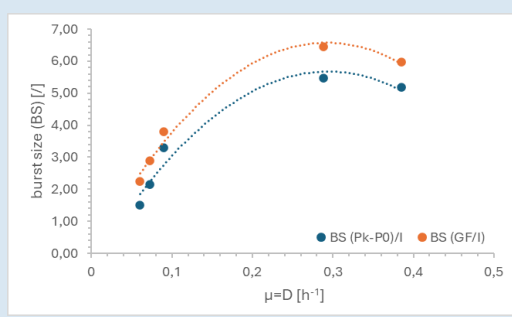


Figure 6: Burst size (calculated in two ways) at different dilution rates

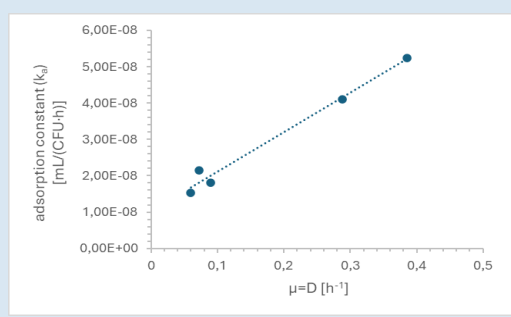


Figure 7: Adsorption constant of bacteriophage K at different growth rates of *S. capitis*

## REFERENCES

- [1] K. Šivec, A. Podgornik: Determination of Bacteriophage Growth Parameters under Cultivating Conditions. *Appl Microbiol Biotechnol* **2020**, *104*, 8949–8960.
- [2] D. Nabergoj, N. Kuzmić, B. Drakslar, A. Podgornik: Effect of Dilution Rate on Productivity of Continuous Bacteriophage Production in Cellstat. *Appl Microbiol Biotechnol* **2018**, *102*, 3649–3661.
- [3] P. Žnidaršič Plazl, A. Pavko: Praktikum Iz Biokemijskega Inženirstva. Ljubljana: UL, Fakulteta za kemijo in kemijsko tehnologijo 2005.

During the exponential growth phase, *S. capitis* exhibits a maximum specific growth rate of 0,6602 h<sup>-1</sup> (Figure 2). At lower dilution rates, bacterial concentration remains stable (Figure 3), but as the dilution rate nears the maximum growth rate, it decreases, approaching washout conditions. Even in suboptimal states, *S. capitis* remains susceptible to phage infection, with phage concentration increasing up to a dilution rate of 0,288 h<sup>-1</sup> (Figure 4). In the absence of infection, the initial phage concentration ( $P_0$ ) would be equal to the generated phage concentration (GB). Both bacterial and phage dynamics remain relatively stable (Figure 5), despite changes in the physiological state. Improved bacterial conditions enhance phage production (BS) (Figure 6) and increase the adsorption constant at higher dilution rates (Figure 7).

## CONCLUSION

Improved bacterial physiological states enhance phage production and adsorption rates, highlighting the critical role of growth conditions in optimizing phage therapy. Future experiments with intermediate dilution rates between 0,09 and 0,288 h<sup>-1</sup> will be necessary to gather a more comprehensive dataset for better analysis.

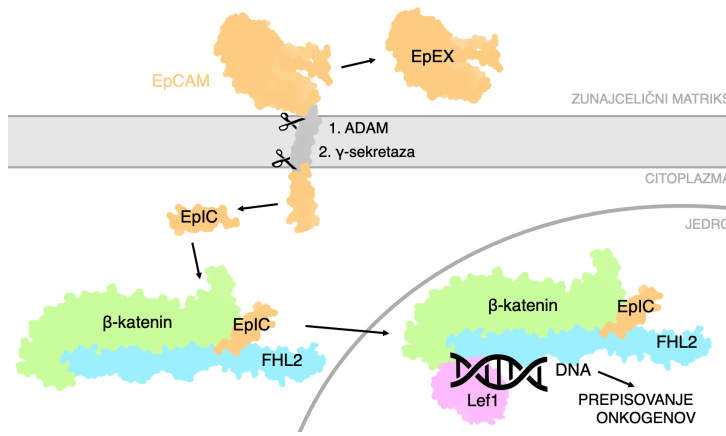
# Raziskovanje strukture signalnega kompleksa FHL2:β-katenin v povezavi z EpCAM

Tina Logonder, Aljaž Gaber

Oddelek za kemijo in biokemijo, Fakulteta za kemijo in kemijsko tehnologijo, Univerza v Ljubljani  
Večna pot 113, 1000 Ljubljana, Slovenija

## UVOD

Epiteljska celična adhezijska molekula (**EpCAM**) je transmembranski glikoprotein pomemben pri morfogenezi epitelia in karcinogenezi epithelialnih celic. Je eden najpogosteje uporabljenih diagnostičnih označevalcev za karcinome. Po cepitvi EpCAM-a se sprosti topna znotrajcelična domena (**EpIC**: aa 289–314), ki tvori signalni kompleks s proteinoma FHL2 in β-katenin v kanonični signalni poti *Wnt*. To vodi do izražanja onkogenov in posledično proliferacije rakavih celic (slika 1). Kljub terapevtskemu interesu je strukturnih informacij o tem kompleksu malo (slika 2). Glavna omejitev dosedanjih študij je bila, da je bil FHL2 v prejšnjih raziskavah izražen kot fuzijski protein z oznako. Namen dela je **strukturalna karakterizacija signalnega kompleksa FHL2:β-katenin z in brez vezanega proteina EpIC**, kar bi prineslo vpogled v mehanizem karcinogeneze proteina EpCAM in razkrilo nove tarče za zdravljenje raka.



Slika 1: Shematski prikaz signalne poti proteina EpCAM, ki se začne z regulirano znotrajmembransko proteolizo (RIP).

## PREDHODNE RAZISKAVE

### Interakcija EpIC:FHL2

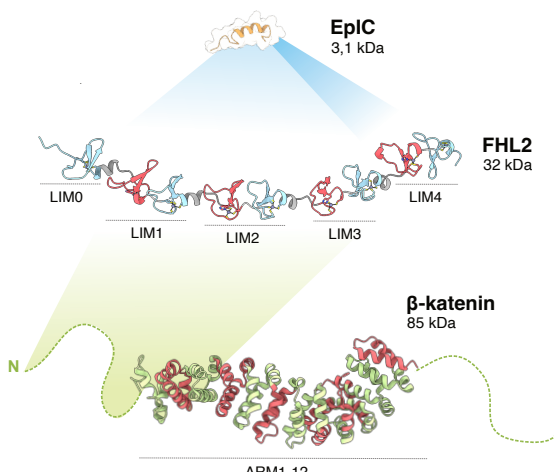
Y2H, Co-IP, SEC:

- vezava EpIC-a na LIM4 FHL2 (Maetzel, 2009)

### Interakcija FHL2:β-katenin

Y2H, Co-IP:

- vse štiri domene LIM (razen LIM0) nujne za vezavo na β-katenin
- vezava FHL2 na N-konec β-katenina (Martin, 2002; Wei, 2003)

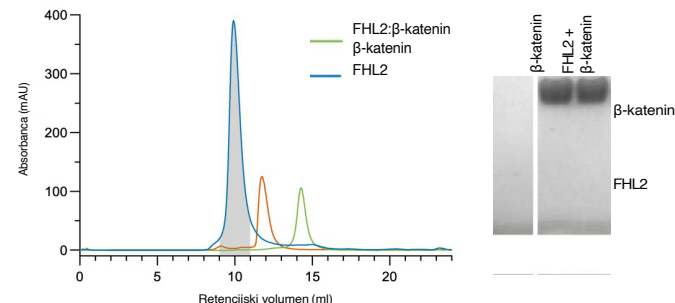


Slika 2: Shematski prikaz interakcij znotraj signalnega kompleksa EpIC:FHL2:β-katenin.

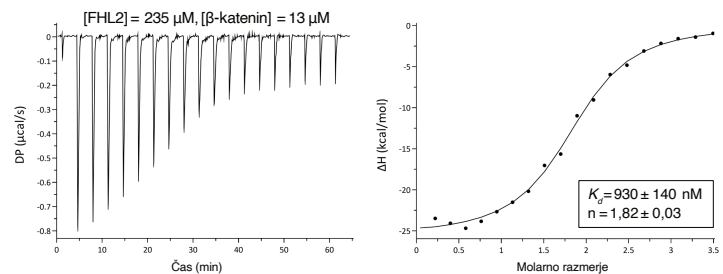
## REFERENCE

1. Gires, O., Pan, M., Schmitz, H., Crone, M., & Baeuerle, P. A. Expression and function of epithelial cell adhesion molecule EpCAM: where are we after 40 years? *Cancer Metastasis Rev.* **39**, 969–987 (2020).
2. Hatabu, J., Clemente-Olivio, M. P., & de Vries, C. J. How (epi)genetic regulation of the LIM-domain protein FHL2 impacts multifactorial diseases. *Cancer* **10**, 2611 (2021).
3. Shang, S., Hua, F., & Hu, Z.-W. The regulation of β-catenin activity and function in cancer: therapeutic opportunities. *Oncotarget* **8**, 33972–33989 (2017).
4. Valenta, T., Haussmann, G., & Basler, K. The many faces and functions of β-catenin. *EMBO J.* **31**, 2714–2736 (2012).
5. Cao, C. Y., Mok, S. W.-F., Cheng, V. W.-S., & Tsui, S. K.-W. The FHL2 regulation in the transcriptional circuitry of human cancers. *Gene* **572**, 1–7 (2015).
6. Cao, C. Y., Mok, S. W.-F., Cheng, V. W.-S., & Tsui, S. K.-W. The FHL2 regulation in the transcriptional circuitry of human cancers. *Gene* **572**, 1–7 (2015).
7. Treiter, J. Innovative therapy modalities for solid EpCAM-positive tumors. (Ludwig-Maximilians-Universität München, 2017).
8. Trzpis, M., Bremer, E., McLaughlin, P. M. J., De Leij, L. F. M. H., & Harmsen, M. C. EpCAM in morphogenesis. *Frontiers in Bioscience* **13**, (2008).
9. Maetzel, D. et al. Nuclear signalling by tumour-associated antigen EpCAM. *Nat. Cell Biol.* **11**, 162–171 (2009).
10. Martin, B. et al. The LIM-only protein FHL2 interacts with beta-catenin and promotes differentiation of mouse myoblasts. *J. Cell Biol.* **159**, 113–122 (2002).
11. Wei, Y. et al. Identification of the LIM-only protein FHL2 as a co-activator of beta-catenin. *J. Biol. Chem.* **278**, 5189–5194 (2003).

## REZULTATI



Slika 3: Analiza interakcije med proteinoma FHL2 in β-katenin z velikostno izključitveno kromatografijo. Levo: kromatogram z vzorci β-katenin + FHL2, β-katenin and FHL2. Desno: analiza frakcij, ki so na kromatogramu označene s sivo barvo, z SDS-PAGE.

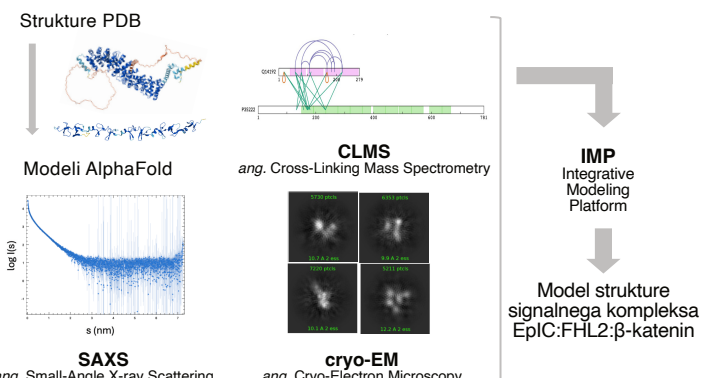


Slika 4: ITC meritev titracije FHL2 v β-katenin. Levo: graf odvisnosti diferencialne moči (DP) v odvisnosti od časa. Desno: graf po integraciji površin vrhov v normalizaciji prikazuje spremembu entalpije v odvisnosti od molarnega razmerja FHL2/β-katenin.

1. Prvič uspešno izražen in očiščen protein FHL2 brez oznake
2. Analiza s SEC (velikostna izključitvena kromatografija): potrjena tvorba stabilnega kompleksa FHL2:β-katenin (slika 3)
3. ITC (izotermna titracijska kalorimetrija) in SLS (statično sipanje svetlobe): stehiometrija FHL2:β-katenin = 2:1
4. ITC:  $K_d$  v mikromolarnem območju (slika 4)

## NADALJEVANJE RAZISKAVE

### Določitev strukture kompleksa EpIC:FHL2:β-katenin s pristopom integrativne strukturne biologije



## ZAHVALA

Delo je bilo podprtlo s strani Javne agencije za znanstvenoraziskovalno in inovacijsko dejavnost Republike Slovenije, raziskovalni program P1-0140 in raziskovalni projekt Z1-2637.

# In vitro antioxidant activity and total phenolic content of different extracts of Himalayan Balsam (*Impatiens glandulifera* Royle)

University of Ljubljana



Marcel Žafran<sup>a,b</sup>, Ana Gajic<sup>c</sup>, Lovro Žiberna<sup>c</sup>, Alen Albreht<sup>a</sup>

<sup>a</sup>National Institute of Chemistry, Department of Analytical Chemistry, Laboratory for Food Chemistry, Hajdrihova 19, SI-1001 Ljubljana, Slovenia

<sup>b</sup>Faculty of Chemistry and Chemical Technology, University of Ljubljana, Večna pot 113, SI-1000 Ljubljana, Slovenia

<sup>c</sup>Faculty of Pharmacy, University of Ljubljana, Aškerčeva cesta 7, SI-1000 Ljubljana, Slovenia

## INTRODUCTION

Himalayan Balsam (HB) is a large annual plant (therophyte) that is classified as an invasive alien plant species. It is considered one of the most virulent plants in Europe and elsewhere in the world, as it is one of the main causes of biodiversity loss. As a result, alternative uses are being sought [1].

At the molecular level, HB is known to contain several compounds of academic and industrial interest [2]. It has been suggested that extracts of *Impatiens* species could be used as natural sources of antioxidants. Several studies have indicated that certain HB extracts could have some degree of antioxidant activity, but the main contributing compounds have not been identified in these mixtures. It is assumed that phenolic compounds (polyphenols) are at least partially, if not largely, responsible for the observed biological activity [3].

## PURPOSE OF THE RESEARCH

This paper reports preliminary results on the *in vitro* antioxidant activity of HB extracts. Given the considerable number of possible different HB extracts, chemical characterization was performed to determine the total phenolic content (TPC).

## EXPERIMENTAL METHODS

HB extracts were obtained by maceration with three different solvents (ethanol (EtOH), water (H<sub>2</sub>O) and acetone) at three extraction temperatures (room temperature (RT), 50 °C and 70 °C) where possible. Otherwise, the extracts were obtained at RT and under reflux. The extracts were prepared at a ratio of 1:100 to 1:100 000. *In vitro* antioxidant properties were determined by a combination of complementary colorimetric assays (DPPH, ABTS and FRAP). The TPC determination based on the Folin-Ciocalteu reagent was also carried out spectrophotometrically.

## RESULTS

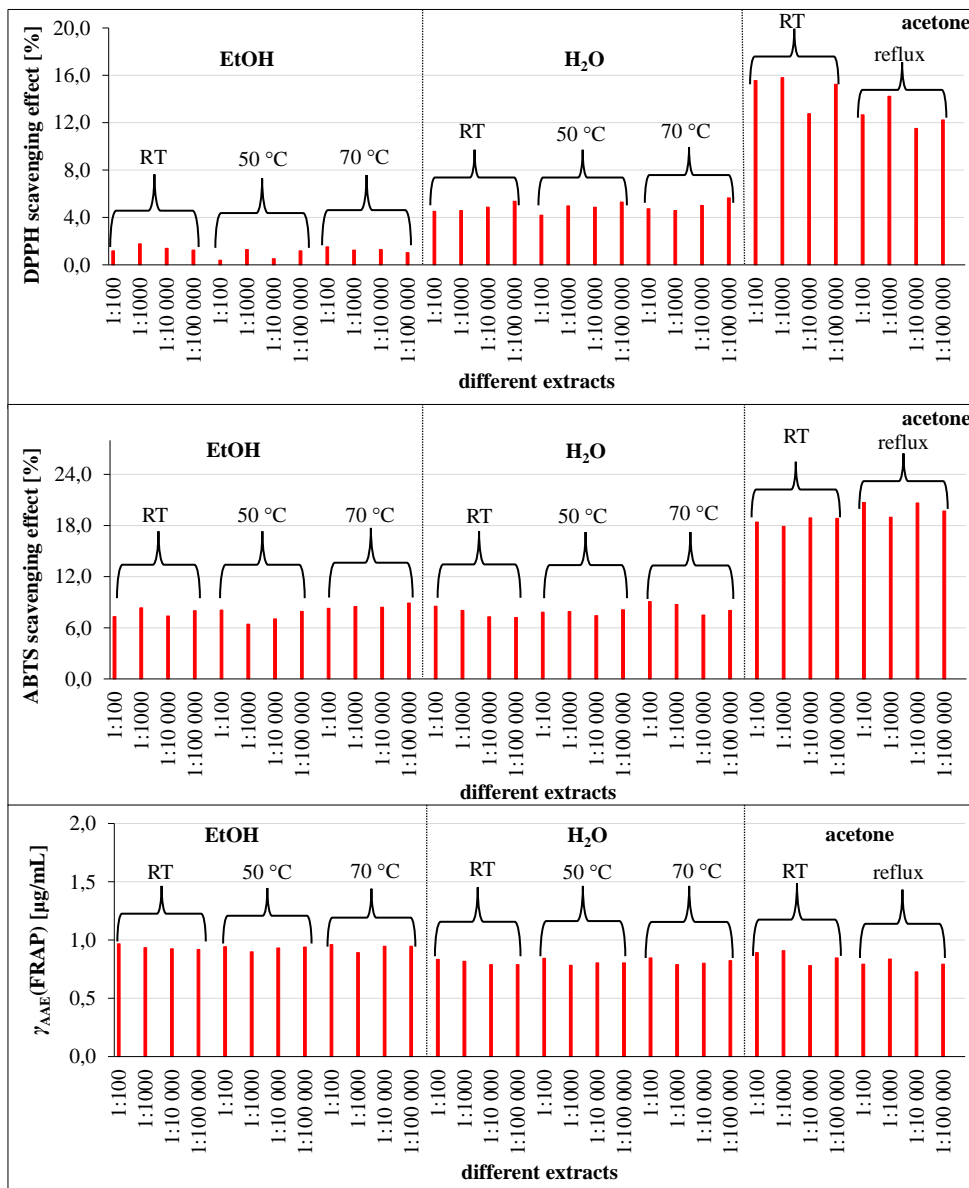


Fig. 1. *In vitro* antioxidant properties of HB extracts of the whole plant. The abbreviation AAE stands for ascorbic acid equivalent.

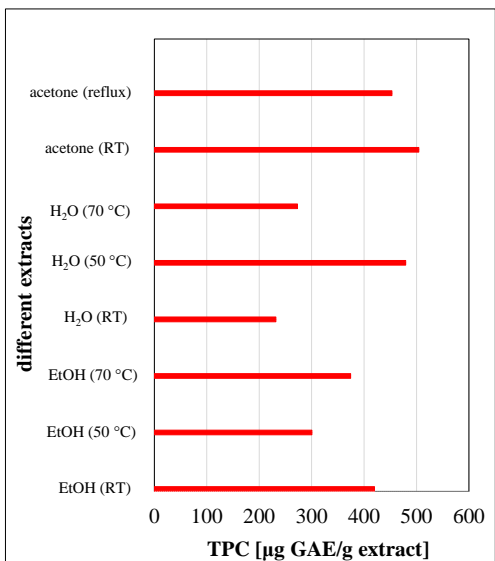


Fig. 2. Determination of the TPC of EtOH, H<sub>2</sub>O and acetone extracts, expressed in  $\mu\text{g}$  of gallic acid equivalent per g of extract.

## CONCLUSIONS

The results of all three *in vitro* antioxidant assays (Fig. 1) showed weak antioxidant activity of the extracts tested. The presence of TPC (Fig. 2) was detected in all extracts tested. Their concentrations ranged from 231.74 to 504.37  $\mu\text{g}$  GAE/g extract. Since phenolic compounds are considered potent antioxidants, we will perform further *in vitro* measurements of antioxidant properties in the future by increasing the amount of plant material or decreasing the amount of extraction solvents used, as we conclude that the extracts obtained in this case were not sufficiently concentrated. We will also perform a more detailed chemical characterization of the extracts to determine which group of compounds contributes the most to their antioxidant activity.

## REFERENCES

- [1] M. Langmaier et al., (2020), A Systematic Review of the Impact of Invasive Alien Plants on Forest Regeneration in European Temperate Forests, *Front. Plant Sci.*, 11, 524969.
- [2] K. Helsen et al., (2021), Biological flora of Central Europe: *Impatiens glandulifera* Royle, *Perspect. Plant Ecol. Evol. Syst.*, 50, 125609.
- [3] V. B. Schini-Kerth et al., (2011), Vascular Protection by Natural Product-Derived Polyphenols: *In Vitro* and *In Vivo* Evidence, *Planta Med.*, 77, 1161–1167.

# Analysis of Adhesive Joint Using Beech Wood

Tjaša Likeb,<sup>1</sup> Martin Capuder\*,<sup>2</sup> Tina Skalar,<sup>1</sup> Andreja Podelak<sup>2</sup>

<sup>1</sup> Faculty of Chemistry and Chemical Technology, University of Ljubljana, Večna pot 113, SI-1000 Ljubljana, Slovenia, [t18013@student.uni-lj.si](mailto:t18013@student.uni-lj.si)

<sup>2</sup> Slovenian national building and civil engineering institute, Dimičeva ulica 12, 1000 Ljubljana, Slovenia

## INTRODUCTION

Wood is an anisotropic, porous material with key features like longitudinal tracheids in softwoods and vessel elements in hardwoods, facilitating resin flow. Glue is the primary bonding material in wood products, with adhesives classified as organic, semi-synthetic, or synthetic.

## MATERIAL & METHODS

Samples were prepared with two compression times (60 min, 120 min) and three wood ring orientations: radial-radial (RR), radial-tangential (RT), and tangential-tangential (TT). Polyurethane glue (PUR) was used. The samples were exposed to UV radiation and moisture for 3 months.

The shear strength (EN302) and microstructure (by optical microscope, SEM, EDS, FTIR, XRD, and epifluorescence microscopy) were analyzed.

## PENETRATION DEPTH (t = 0)

Table 1: Adhesive joint thickness and depth of penetration of the adhesive into the wood microstructure (annual rings orientation: RR, TT)

	RR		TT	
	60 min	120 min	60 min	120 min
Adhesive joint thickness [µm]	128.2	75.8	97.2	45.6
Penetration into the bottom plate [µm]	339.8	37.9	324.5	85.5
Penetration into the upper plate [µm]	25.8	478.6	77.9	110.2

Table 2: Adhesive joint depth of penetration of the adhesive into the wood microstructure by area by plates (annual rings orientation: RR, TT)

Orientation	A(P1) [%]	A(P2) [%]
RR	70,17	29,83
TT	38,72	61,28

	RT		
	60 min	120 min	A(P1) [%]
Adhesive joint thickness [µm]	253.9	8.3	/
Penetration into R oriented plate [µm]	22.9	299.2	84.38
Penetration into T oriented plate [µm]	89.6	140.4	15.62

Table 3: Adhesive joint depth of penetration of the adhesive into the wood microstructure by distance and by area by plates (annual rings orientation: RT)

## RESULTS

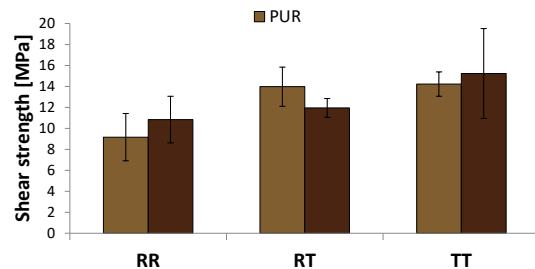


Figure 1: Shear strength results

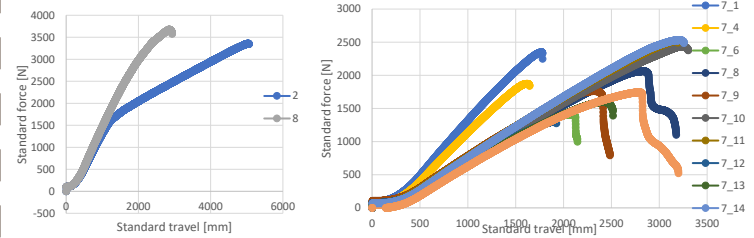


Figure 2: Tensile-shear test results for the samples before and after aging (1 month)

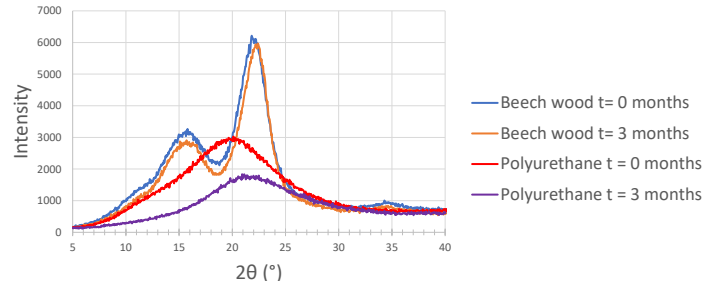


Figure 3: XRD results for beech wood and polyurethane glue analysis before and after aging

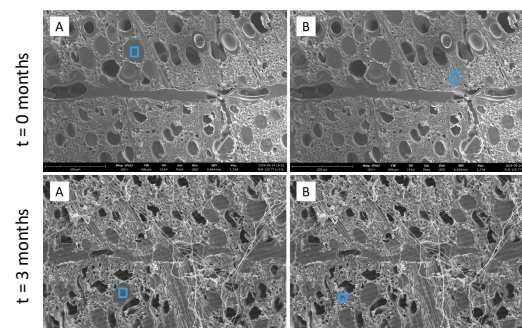


Figure 4: SEM image of a sample PUR 120 TT (time of aging: 0 and 3 months, A – polyurethane glue, B – beech wood)

## CONCLUSION

This study focuses on the aging process of wood joints, essential for understanding the durability of wooden structures. We investigated how environmental factors like moisture, temperature changes, and mechanical stress affect wood over time. Our results showed that samples compressed for 120 minutes with radial-tangential (RT) orientation had the best penetration. To fully assess aging effects, prolonged exposure is necessary, as both wood and polyurethane glue degrade over time. Identifying weaknesses through this research supports the development of stronger joint designs and the selection of more resilient materials, enhancing the longevity of wooden constructions.

Partnerji dogodka **BEST** dnevi znanosti:

*Diamantni partner*

**SANDOZ**



**lek**

*Zlati partnerji*

**KRKA** | 70

**PIPISTREL**  
BY TEXTRON eAVIATION

**GEN**  
SKUPINA

**NOVARTIS**

 TEHNOLOŠKI PARK  
LJUBLJANA  
01

**PORTON**  
Porton PharmaTech, d.o.o.

*Srebrni partnerji*

**METRONIK**

**NIB** NACIONALNI INSTITUT ZA BIOLOGIJO  
NATIONAL INSTITUTE OF BIOLOGY

 Institut  
"Jožef Stefan"  
Ljubljana, Slovenija

 IXTLANTEAM



*Soorganizatorja:*

 **FKKT**  
UNIVERZA  
V LJUBLJANI  
Fakulteta za kemijo  
in kemijsko tehnologijo

 **FRI**  
UNIVERZA  
V LJUBLJANI  
Fakulteta za računalništvo  
in informatiko